surgery remains the cornerstone treatment approach to this disease. The development of lymph node metastasis is a well-established independent risk factor for recurrence of gastric cancer. In recent years, two independent research groups have established microarray based risk factor scoring systems for the development of lymph-node metastasis in gastric cancer. In 2002, a Japanese group published a study in patients with Intestinal Type Gastric Cancer [Hasegawa 2002]. Primary gastric cancer and corresponding non-cancerous gastric mucosa from 20 patients who underwent surgery were comparatively analyzed. A set of 61 genes that were commonly upregulated and 63 genes downregulated in Intestinal-Type Gastric Cancer in more than 75% of the cases could be identified. In a second step, the expression profiles of nine cases with and cases without lymph-node metastasis were compared. In this approach, 12 genes that were differentially expressed (P<0,01) could be identified by employing a random permutation test. Nine of these 12 genes were overexpressed and three were downregulated in node positive tumors. By use of a "stepwise discriminant analysis", five independent "predictors" were identified among these 12 genes (Table **6**). The predictive scoring system was confirmed in nine independent additional tumor tissue samples. All nine cases (four node positive and nine node negative) were correctly assigned to each class by means of the scoring system.

One year later, a Dutch group performed a comparable investigation. The molecular data of 35 gastric carcinomas were analyzed with their clinical data sets [Weiss 2003]. Microarray Comparative Genomic Hybridization (GCH), which allows to analyze accumulation of genetic changes that to a large extent occur on a chromosomal level, was applied to their approach. Three different groups could be distinguished by "hierarchical clustering" of the microarray CGH results. For each cluster, they could define a signature of 204 genes by using a "leave one out" cross validation. Each cluster was analyzed for correlation with clinico-pathological data. The lymph–node status and the overall survival were criteria with significant differences between the individual groups. In one group, significantly less lymph-node positive cases (40%) were found than in the ones (83% and 88%). Patients who belong to the former group were found to have a significantly longer survival duration (P=0,019).

Both cited studies focussed on a clinically most important issue. The discussion about the inclusion of extended lymph node dissection into surgery for gastric cancer remains rather controversial [Bonenkamp 1999, Cuschieri 1999]. The increase of overall morbidity and mortality associated with this treatment strategy has to be well-balanced against the benefit for lymph-node positive patients following this intervention. Predicting the overall risk of lymph-node metastasis by microarray techniques in an individual patient could be a reasonable strategy to select patients for this kind of therapy in the future and would have major implications for the clinical practice in this entity.

In 2003, Suganuma published a study focussed on possible chemoresistance-related genes in gastric cancer [Suganuma 2003]. Tumor samples and corresponding normal mucosa from 35 patients with advanced gastric cancer were differentially examined. The *in vitro* sensitivity of cells from each dissociated tumor sample against cisplatin, 5-flourouracil, mitomycin C and doxorubicin was measured by MTT (4,5-dimethylthiazol-2-yl)-2,5-diphenyltetrazolium bromide) assay. The results obtained from in-vitro cytotoxicity testing assays were correlated with the results of cDNA microarray analysis of corresponding tissue samples. In the case of cisplatin, "hierarchical clustering" could successfully distinguish "sensitive" and "resistant" tumors from each other. A set of 23 potential "cisplatin-resistance-related-genes" could be selected by this method. The latter group included vascular permeability factor, two membrane-transporting subunits and retinoblastoma-binding protein. In a further selection based on strong criteria, metallothionein IG and heparin-binding-epidermal-growth-factor-like-growth factor were also identified as candidates for cisplatin-resistance-related genes. Within this approach, dihydro-pyrimidine dehydrogenase and HB-EGF-like growth factor were suggested to be 5-FU resistance-related genes. In this innovative approach, the authors could demonstrate that DNA-microarray could be useful to investigate drug-resistance and would be a means to understand some of the complex mechanisms behind it. Although this study is only based on a limited data set, this method could in principal be an important step for an individualized and customized cancer therapy in the future.

Moreover, in 2003, a Japanese group published a correlative study based on gene expression profiling in patients with colorectal cancer [Tsunoda 2003]. To clarify the regulatory factors in this malignant disease, differential gene expression profiles were analyzed by filter-array in

Table 6. Five Genes for Predicting Risk of Lymphnode Metastasis in Intestinal Gastric Cancer (Hasegawa 2002)

Title		Discriminant coefficient
DDOST	dolichyl-diphosphooligosaccharide-protein glycosyltransferase	1.87
GNS	glucosamine (N-acetyl)-6-sulfatase (Sanfilippo disease IIID)	1.26
NEDD8	neural precursor cell expressed, developmentally down-regulated 8	1.29
LOC51096	CGI-48 protein	1.36
AIM2	absent in melanoma 2	-1.54

Five genes were selected based on microarray data for predicting risk of lymph-node metastasis in intestinal gastric cancer (Hasegawa 2002).This "predictor" was validated in 9 additional independent cases. All cases were (four node positive and five node negative) were assigned to each classes.

surgically resected specimen (tumor and normal mucosa) obtained from ten patients with colorectal cancer. The correlation between several clinico-pathological factors and cancer-related genes were investigated by using complex statistical analyses including "average linkage hierarchical clustering and principal component analysis (PCA)[3]". As an example, the c-myc-binding-protein and the c-jun-proto-oncogene were both identified as possible correlative markers for histological differentiation and overall clinical prognosis (Fig. (3)). The early-growth-response-protein 1 was selected to play an important role in the progression of clinical stage. The authors concluded that PCA was identified as an appropriate method to select candidate genes relevant to predict clinico-pathological factors in a small population of clinical samples from colon cancer patients.

LYMPHOMA

Diffuse large B-cell lymphoma (DLBCL) represents the most common subtype among the lymphoid neoplasm in adults (International Lymphoma Study Group 1997). Less than 50% of the patients are currently cured with standard combination chemotherapy [Popat 1998]. In 2000, the first large gene expression profiling study was performed in this disease [Alizedah 2000]. Within this study, different types of diffuse large B-cell lymphoma patients could be identified by gene expression profiles. A specific microarray assay for lymphoma was designed. This "Lymphoma-chip" included genes preferentially expressed in lymphoid cells and genes with known or suspected roles in cancer development and immunology. Using this array, 96 normal and different malignant lymphocyte samples were comparatively

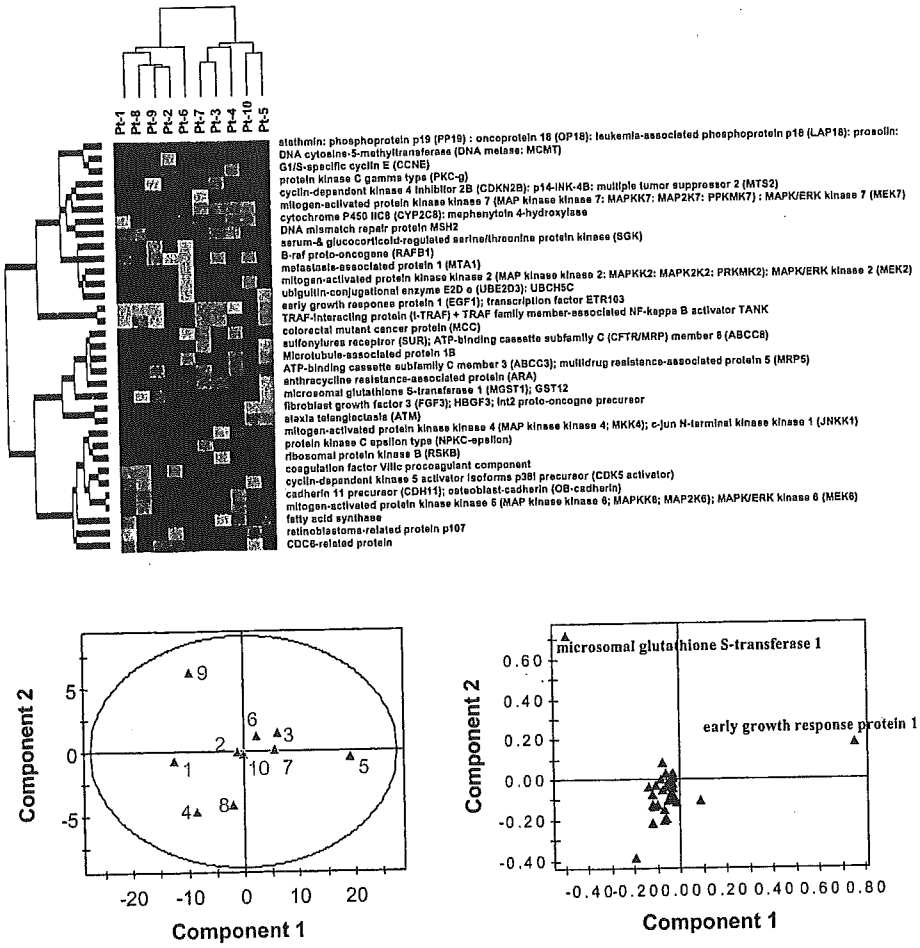

Fig. (3). (A). Average-linkage hierarchical clustering analysis of ten colorectal tumor samples on histological diagnosis. Right cluster shows the group of the well-differentiated and left shows the group of the other differentiations. (B) Principal component analysis on histological diagnosis. The numbers in blue indicate the patients with well-differentiated adenocarcinoma and the numbers in red indicate the patients with the other differentiations. The c-myc binding protein gene and the c-jun proto oncogene were identified as possible markers for histological differentiation.

analyzed. All DLBCL samples could clearly be separated from normal lymphocyte samples and other lymphomas. Focused on genes related to a separate stage of B-Cell differentiation and activation, a germinal-centre-B-like

[3] **Principal component analysis:** A method of analyzing multivariate data in order to express their variation in a minimum number of principal components or linear combination of the original, partially correlated variables.

DLBCL and an *in vitro*-activated-B-like DLBCL could be distinguished among the group with diffuse large B-cell lymphoma by "hierarchical clustering" analysis. This clustering was based on the hypothesis that DLBCL derives from normal B-cells within the germinal centres (GC). As a consequence to this, overall survival and clustering to one of these two groups were correlated. Patients belonging to the GC-B-like-group had a significantly higher five-year survival rate than patients belonging to the activated-B-cell-DLBCL group (P< 0,01). The average five-year survival rate for all patients was 52%, for patients of the GC-B-like DLBCL was 76% and for patients of the activated B-like DLBCL only was found to be 16%. Two years later, Shipp and co-workers published another prognostic score for DLBCL based on gene expression profiling [Shipp 2002]. Contrary to the latter work, an alternative strategy that was independent of an *a priori* hypothesis was employed. A novel "supervised learning method" was applied. Tumor samples from 77 patients were analyzed. 58 patients with DLBCL and 19 patients with Follicular Lymphoma were clearly distinguishable by the use of this method. Clinical outcome prediction in DLBCL patients based on gene expression profiling data was the further purpose of this study. The long-term follow up was available for all DLBCL patients. While 32 patients were eventually cured, 26 patients turned out to have fatal or refractory lymphoma disease. An "outcome predictor" was designed using a "supervised learning classification approach" (weighted voting algorithm and cross validation test). The highest accuracy was obtained using a "predictor" set of 13 genes (Table 7). Using this "predictor" set, the DLBCL collective could be divided into a *"cured"* and on the other hand, a *"fatal and refractor"* group. The Kaplan Maier survival analysis revealed a significantly better 5-year-overall-survival rate for the *"cured"* group with 70% in comparison to the *"fatal and refractory"* group with 12% (P=0.00004). Based on these results, their model was validated in the dataset from the previously mentioned study. A set of 90 genes was represented in their cDNA microarray as well as in the oligonucleotide microarray (*lymphoma-chip*) employed by Alizedah. Both patient groups could be divided in the two *"cell of origin"* groups classified by Alizedah using this 90 gene set. This *"cell of origin"* differential analysis distinction was strongly associated with clinical outcome in the dataset of Alizedah but not in the actual patient group of DLBCL. Furthermore, the predictive power of their own 13 gene based "predictor" was tested in the dataset of Alizedah. Three of these genes were represented in the *"lymphoma-chip"* of Alizedah: NOR1, PDB4B and PKCβ. Significant correlation with outcome was found for NOR1 (p=0,05) and PDB4B (p=0,07). Results for PKCβ were discordant by representing multiple cDNAs on the *"lymphoma-chip"*. These results suggest a significant advantage for a "supervised learning method for the prediction of clinical outcome of disease" in comparison to the "unsupervised hierarchical clustering". The same dataset of Alizedah was re-analyzed by a Japanese group [Ando 2002]. "Fuzzy Neural Network[4]" as a new statistical method to analyze prediction power of gene expression was applied in their investigation. Their model identified four genes (CD 10, AA807551, AA805611 and IRF-4) that could be used to predict prognosis with 93% accuracy.

Table 7. Model of 13 Genes Predicting Outcome in DLBCL Patients (Shipp 2002)

Genes associated with good outcome	Genes associated with poor outcome
-Dystrophin related protein 2	-H731
-3UTR of unknown protein	-Transduction like enhancer protein 1
-uncharacterised	-PDE 4 B
-Protein Kinase C gamma	-uncharacterised
-Minor / NOR 1	-Protein kinase C beta 1
-Hydroxitryptamine 2B Receptor	-Oviductal glycoprotein
-Zinc finger protein C2H2-150	

A 13-gene based "predictor" for outcome in DLBCL patients was developed based on microarray data by a supervised learning method (Shipp 2002). The expression of seven genes were associated with good and the expression of six genes was associated with poor outcome. This "predictor" was superior to "hierarchical clustering" based classification of Alizedah in predicting outcome of DLBCL patients.

In 2003, a Japanese cooperative research group published a study in Primary Central Nervous System Lymphomas (PCNL) using Filter-Array Assays [Yamanaka 2003]. Among 21 brain tumor and normal brain tissue samples, six PCNLs could be clearly distinguished by "hierarchical clustering" (Fig. (4)). The genes encoding for Laminin-receptor-2, thioredoxin-peroxidase and elongation-factor-1 were selected by Principal Component Analysis (PCA) as genes specific for PCNSL. The gene expression profiles of the six PCNL samples were correlated with the clinical outcome of the corresponding patients. These six patients could be distinguished into groups on the basis of post-treatment survival, a parameter likely related to response to therapy: group I >24 month (3 cases); group II < 23month (3 cases). All six patients were treated uniformly with the same chemo-radiotherapy regimen. A set of 76 genes capable of distinguishing the treatment sensitive group from the non-sensitive to treatment group was selected by the Whitney-Mann test. Among these 76 genes, 37 genes were found upregulated and 39 genes were found downregulated in responders. Interestingly, 10 of the 37 upregulated genes were involved in angiogenesis, while 6 of the 39 downregulated genes were involved in apoptosis. Using the selected genes related to response to chemo-radiotherapy, re-clustering was performed. The responders and non-responders could successfully be separated on the basis of subtle differences in distribution of gene expression (Fig. (5)). This study represents another example of how genomic techniques may improve evaluation of complex treatment and prognosis evaluation of neoplastic disease.

RELIABILITY AND REPRODUCIBILITY OF ARRAY DATA

These examples of investigations with microarray technique surely represent landmark studies in their

[4] **Fuzzy neural network:** A special kind of artificial neural network.

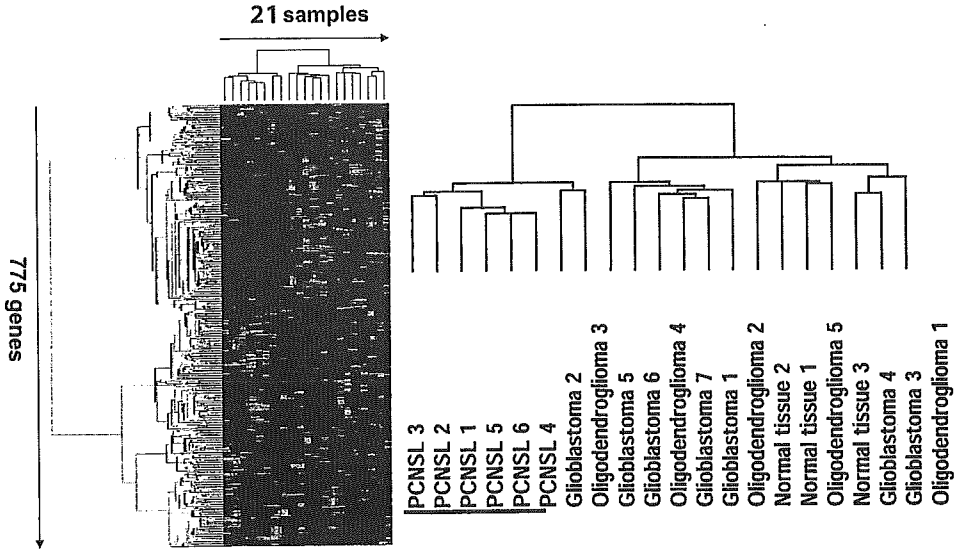

Fig. (4). Macroarray analysis of the 21 samples including PCNSCL, Glioblastoma, Oligodendroglioma and normal tissue. The phylogenetic tree obtained by application of the " clustering algorithm" shows separation of the PCNSL.

individual fields. They have brought a realistic hope to the scientific community that long time open issues will be solved within the near future. But besides all well-founded hope and enthusiasm, it cannot be overlooked that analyzing and interpreting array data remains a rather complex technology. Applying these novel genomic techniques uncritically to clinical data sets and clinical trials could lead to potentially problematic results and conclusions. It has to be critically taken into account that these novel techniques are still experimental. The question of validation and reproducibility remains the major issue. A number of studies regarding these technical and statistical problems have been reported within recent years. We will try to summarize the most important ones of these in the following paragraph.

A fundamental problem for comparing gene expression profiles from different populations or groups (e.g. normal/disease) are large variations between individuals within the same population. It is difficult to distinguish differences in gene expression that appear associated with a specific disease from random genetic variations. Oleksiak has performed a landmark study regarding this important issue for all gene expression based studies [Oleksiak 2003]. Gene expression profiles within and among populations of the teleost fish of the genus Fundulus were analyzed in

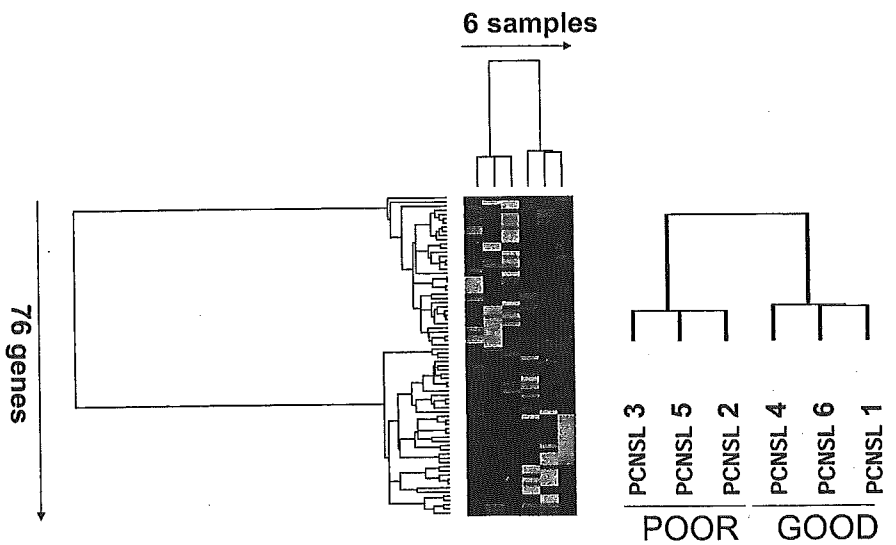

Fig. (5). Re-clustering was performed using selected genes related with response to chemo-radiotherapy.The responders (described as GOOD) and non-responders (described as POOR) were clearly separated clearly by the re-clustering method.

this investigation. Statistically, significant differences in expression profiles between individuals within the same population for approximately 18% of 907 genes were observed. Typically, expressions differed by a factor of 1.5 and often even more than a factor of 2.0. In addition to that, Enard *et al.* found in global comparisons of mRNA-levels of chimpanzee and human brain tissue, greater variations within the human population than between the human and the chimpanzee population [Enard 2002]. Both studies point out the importance to recognize the large variations between individuals within a population in study design as well as in the appropriately selected statistical analysis.

Our group has focussed largely on relevant questions of gene-profiling practice within the recent years. From small tumor samples, often only a small amount of RNA can be obtained. In some cases, this amount is not enough to perform gene profiling assays. Amplification of RNA to a.cRNA (amplificated RNA) is one common way to enlarge the given RNA amount. Possible artificial changes of gene expression influenced by amplification have not yet been examined in detail. A two step amplification method was used in our validation experiment (Fig. (**6**)). By this approach, 10-100 μg amplified cRNA from a small amount of total RNA (1_g or less) could be obtained. Then we have focussed on the question whether differential gene expression is conserved after amplification. The differential gene expression profiles of the PC 14 cell line and a sample of peripheral blood lymphocytes (PBL) were compared using mRNA and after amplification, a.cRNA. Although the R-Ratio was lower, we could conserve significant differences in the gene expression profiles after amplification (Fig. (**7**)). These preliminary results suggest that a gene-profiling study could be based on only small samples with a small amount of RNA if an appropriate amplification would be performed.

Another promising application of genomic techniques is to observe time or dose dependent changes of gene expression profiles in tumor tissue under the influence of a given drug application. However, repeated tumor sampling is necessary. This remains a very encumbering approach for the patient and often not possible in clinical every day practice. Therefore, we have examined, if a more easily performed method to obtain peripheral blood lymphocytes might be useful as a method to identify surrogate tissue for observing drug related changes in gene expression profiles. Within a clinical phase-I study with a novel Farnesyl-transferase Inhibitor, we have collected tumor samples and peripheral blood lymphocytes predose and on days two and eight following drug application (Fig. (**8**)). A cDNA filter-array assay including 775 genes chosen for predicting chemo-sensitivity was used for analyzing gene expression profiles (Fig. (**9**)). Interestingly, changes in gene expression were not only observed in tumor sample but also in the PBL. In still ongoing clinical research, we are currently trying to determine the role of PBL as surrogate tissue in pharmacogenomic cancer research.

In 2002, Churchill presented a basic review article about the fundamentals of experimental design for cDNA microarrays [Churchill 2002]. The appropriate design of a microarray experiment is essential for the scientifically based interpretation of the results. He pointed out the importance to analyze an adequately high number of biological samples to achieve representative, predictive and validated results. A higher number of technical replication with the same biological sample could not lead to validation of the results in most cases. Although the optimal design of an experiment or a study is the basis for successful results, the appropriate statistical analysis of the obtained data turns out to be of further importance too. An inadequate data analysis can lead

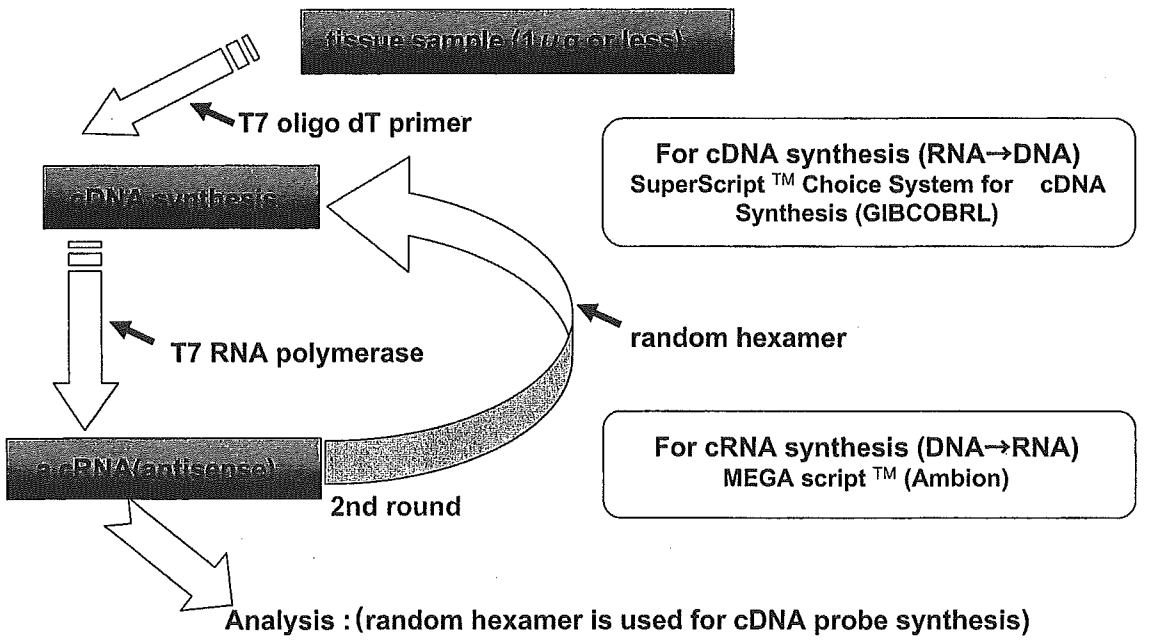

Fig. (6). Gene amplification by T7-based RNA amplification method. In a 2 step approach, first cDNA was synthesized (RNA→DNA) followed by c.a.RNA synthesis (DNA→RNA), we could purify 10-100μg RNA of amplified cRNA from small amount of total RNA (1μg or less).

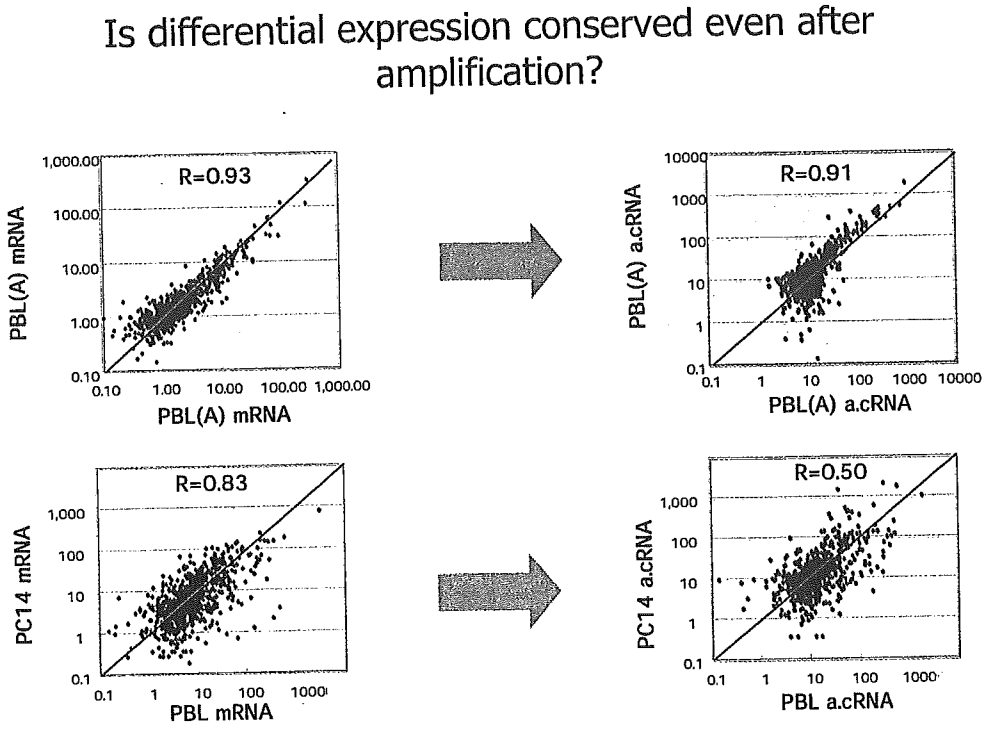

Fig. (7). Is differential expression conserved even after amplification? In order to analyze the reproducibility of the clinical samples, the gene expression profile of non-amplified and amplified samples were compared in scattered plot. Upper: gene expression data of duplicate samples of peripheral blood mononuclear cells were compared in scattered blot. High reproducibility (R=0.93) was obtained. These reproducible profiling was also observed in the amplified samples (R= 0.91). Lower: In a second experiment, we compared the differential gene expression of the PC 14 cell line and of peripheral blood mononuclear cells using mRNA and after amplification a.cRNA (amplified cRNA). Also the reproducible profiling was lower after amplification (R=0.50) than in non-amplified samples (R=0.83); we could conserve significant differences in gene expression after amplification.

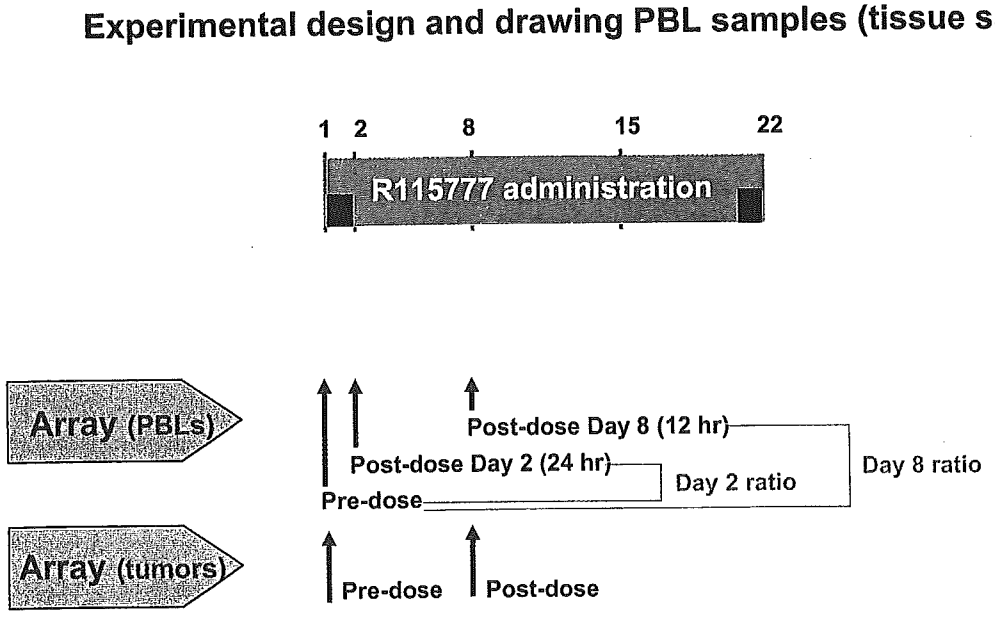

Fig. (8). Experimental design: sampling of PBL and tissue samples in correlative study in clinical phase I study of a falnesyltransferase inhibitor (FTI). Peripheral Blood Lymphocytes and tumor samples were collected predose, postdose day 2 and post dose day 8. Gene alteration after administration of FTI was analyzed for proof the pharmacodynamic effect of FTI.

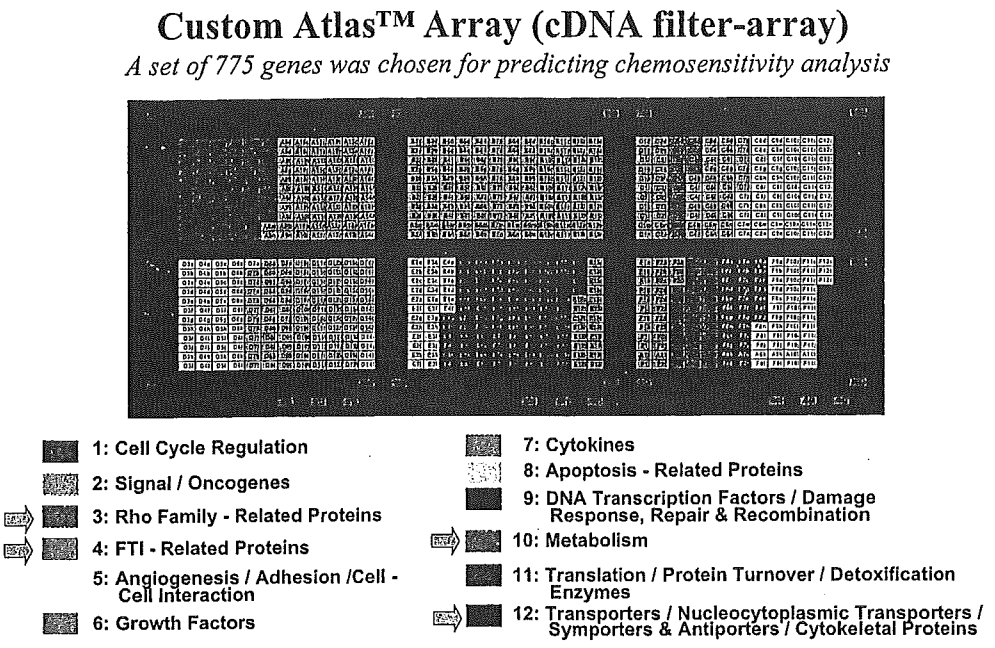

Fig. (9a). The cDNA filter-array with a set of 775 genes chosen for predicting chemosensitivity analysis.

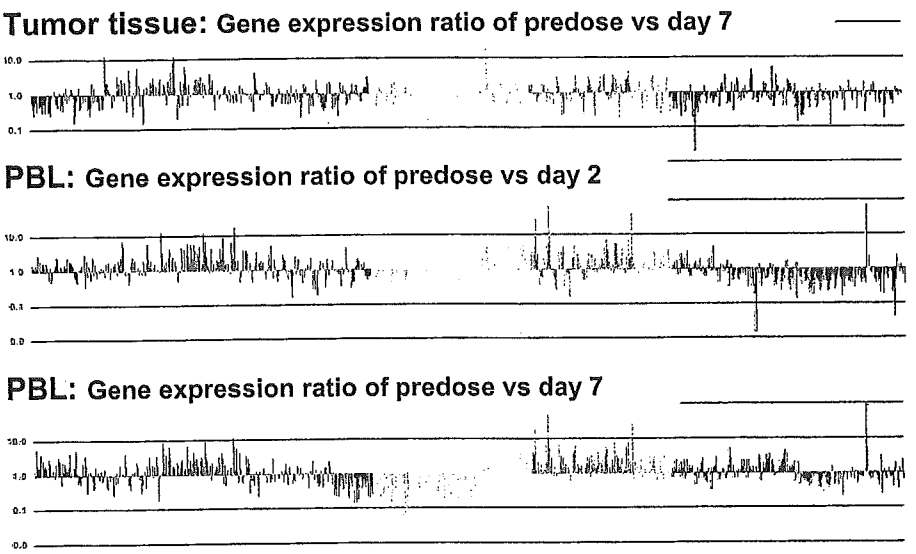

Fig. (9b). Gene expression changes of tumor tissue and PBL in the melanoma patient after administration of FTI. Specific gene groups were modulated by FTI. Changes in gene expression influenced by FTI were not only observed in the tumor samples but also in the peripheral blood lymphocytes. This findings suggest that drug modulated changes of gene expression in peripheral blood lymphocytes could be useful as surrogate markers in pharmacogenomic studies.

to potential pitfalls. As previously shown, the lymphoma data set of Alizedah is analyzed by different groups with different statistical methods, thus leading to partially different or even conflicting results. It is most important to recognize that different purposes of studies require different methods of statistical analyses. For example, the commonly used "unsupervised hierarchical clustering" although useful for discovery subsets in a number of tumor samples within the same histological group, is not appropriate to compare these amongst each other or establish a meaningful "predictor" [Simon 2003]. In 2001, Tusher *et al.* published a new method for analyzing microarray data [Tusher 2001]. In

their investigation, they focussed on the problem to identify significant changes in gene expression profiles between different functional biological states. Cluster analysis provides only little information about statistical significance, and conventional *t* test is not appropriate for the thousands of data obtained within these microarray experiments. This problem led them to develop a statistical method adapted specifically for microarray analysis. This "Significance Analysis of Microarrays (SAM)" assign a score to each gene on the basis of gene expression relative to the standard deviation of repeated measurements. This method was used in the breast cancer study of Sorlie [Sorlie 2001]. Another important challenge is the integration of microarray data generated by different research groups on different array platforms. Moreau has currently summarized three major problems: (1) the efficient access and exchange of microarray data; (2) the validation and comparison of data from different platforms (cDNA and short long oligonucleotides); and (3) the integrated statistical analysis of data sets [Moreau 2003]. Tan has reported a considerable divergence of results from three different commercial available microarray platforms analyzing the same RNA sample [Tan 2003]. The most common application of microarray technology is the prediction of clinical outcome in cancer. The most important reports have been referred to within in the first part of our review. Nitzani and Ioannidis systematically analyzed studies correlating outcome with genetic profiles based on microarray data published from

Table 8. Analysis of Microarray Based Correlation Studies (1999-2003) by Nitzani and Ioannidis (Nitzani 2003)

Characteristic	Studies of major clinical outcomes (n=30)	Other studies (n=54)	Total (n=84)
Year of publication			
1999	1(3%)	2(4%)	3(4%)
2000	2(7%)	1(2%)	3(4%)
2001	6(20%)	18(33%)	24(29%)
2002	18(60%)	28(52%)	46(55%)
2003	3(10%)	5(9%)	8(10%)
Malignant disorder			
Haematological	9(30%)	9(17%)	18(21%)
Solid tumor	21(70%)	45(83%)	66(79%)
Median (IQR) number of samples			
Total	62(29-96)	30(18-44)	37(20-57)
Specific cancer	43(24-69)	20(13-36)	25(15-45)
Microarray type			
cDNA	19(63%)	31(57%)	50(60%)
Oligonucleotide	11(37%)	23(43%)	34(40%)
Median (IQR) number of probes	8683 (6817-18 624)	6936 (4569-12 600)	7014 (5534-12 600)
Training			
Independent	9(30%)	17(32%)	26(31%)
Dependent	8(27%)	20(37%)	28(33%)
Both	13(43%)	17(32%)	30(36%)
Validation			
Independent	3(10%)	1(2%)	4(5%)
Cross-validation	6(20%)	4(7%)	10(12%)
Both	3(10%)	5(9%)	8(10%)
None	18(60%)	44(82%)	62(74%)
Outcomes/correlates assessed			
One	9(30%)	35(65%)	44(52%)
Two to four	12(40%)	11(20%)	23(27%)
Five or more	9(30%)	8(15%)	17(20%)
Significant associations reported			
Yes	21(70%)	20(37%)	41(49%)
No	9(30%)	34(63%)	43(51%)

Microarray correlation studies focused on prediction outcome or other important clinico-pathological features were systematically analyzed by Nitzani and Ioannidis in 2003. This table shows the results of their investigations. In 70% of the studies correlating major clinical outcome with gene expression significant associations were reported. However, in only 30 percent of the major outcome focused studies cross-validation or independent validation was performed. These findings underline the need for consequent quality control and validation in microarray based clinical studies.

1995-2003 [Nitzani 2003] (Table 8). They concluded that the predictive performance of this new technique was variable and in many cases, molecular classifications were not subject to an appropriate validation. Of note is, that they found out that only in 30% of the studies with major clinical implication an appropriate cross-validation or independent validation check was performed.

Another substantial open issue in the proceedings of DNA-microarray techniques in translational cancer research is the lack of information of the concrete biological function of encoding proteins. Most investigators have validated their DNA-microarray results by Real-Time-PCR [Chaqui 2002]. Although we can measure the level of expression of the genes of interest in a reliable way, we will miss information of the post-translational protein modifications, time course of protein expression, conditions of protein synthesis, cellular location of the protein, activation of the protein and interaction with other molecules. Therefore, more and more authors combine in their investigations DNA-techniques as DNA microarray and Real-Time-PCR with non-DNA techniques such as tissue-array, immunohistochemistry and western blotting. White and co-workers published a remarkable study focused on the correlation between mRNA and protein expression [White 2004]. This British group performed a microarray analysis to compare transcription in response to the ErbB-2 receptor tyrosine kinase activity in a model of a mammary luminal epithelial cell system. They compared the differences of mRNA expression with changes at protein level using a parallel proteomic strategy employing two-dimensional difference gel electrophoresis (2-D-DIGE) and quantification of multiple immunoblotting experiments. Interestingly, they found a high correlation between transcription and translation for the subset of genes studied. Moustafa and colleagues include immunoblotting in the validation of their DNA microarray experiment [Moustafa 2002]. To identify genes involved in head and neck cancer, they compared the gene expression profile in matched primary normal epithelial cells and primary head and neck cancer cells from the same patients employing a cDNA microarray consisting of 12530 genes human genes. They found significant changes in the expression of 213 genes. 91 genes were found upregulated and 122 downregulated in the cancer-cells. In general, most of the genes that are overexpressed in the head and neck cancer cells encode for growth factors and cell structure. The underexpressed genes are involved in cell-cell adhesion and motility, apoptosis and metabolism. To validate their results at protein level, they investigated the expression of nine selected genes from the cell-cell adhesion and motility group by immunoblotting and Reverse Transcriptase-PCR. They found in three of the four cell line pairs consisting results of DNA-microarray, Reverse Transcriptase–PCR and immunoblotting. However, in one sample, they found conflicting results between the protein and the mRNA expression of E-cadherin and γ-catenin. These differences may be explained by differing rates of translation or protein stability in the cancer cell versus their normal counterparts. Tissue microarrays (TMA) are promising approaches for validation of DNA-microarray results [Chaqui 2002, Hao 2004, Mousses 2002]. A TMA is a slide with dozens to hundred predefined microscopic sections of tissue. This makes it feasible for an investigator to measure DNA, mRNA and protein expression in a large number of samples, providing enough statistical power for meaningful analysis. Immunohistochemistry is the most common method applied to TMAs, but *in situ hybridization* is increasingly used. In spite of many clear advantages for TMAs in the validation of microarray results, this technique is not without any limitations. The critical issues involve sensitivity and lack of quantification.

SUMMARY

In summary, these new techniques will play an important role in future of translational cancer research. However, a consequent and critical evaluation is definitely needed. An internationally commonly accepted standardization must be established. Public microarray databases should allow critical comparisons of independent experiences within the same malignant tumor entity. [Stoeckert 2002]. Published investigations should in detail report all key features of the experimental design, the samples used, the extract preparation and labeling performed, hybridization procedures and variables employed, measurement data and specifications generated. Future studies should generally be performed on the basis of the recommendations proposed by the Microarray Gene Expression Database Group (MEGD) [Brazma 2001].

In spite of many unsolved issues, genomic techniques have taken translational cancer research a significant step forward. In some cancer types such as lymphomas and solid tumors, more detailed and biologically relevant risk classifications could be developed using these novel techniques. For several anticancer agents, significant knowledge about mechanisms of action and resistance could be gained. As a consequence to this, genomic techniques will eventually become the backbone of translational cancer research in the upcoming future.

ACKNOWLEDGEMENTS

This work was partially supported by funds for the Third Term Comprehensive 10-Year Strategy for Cancer Control and a Grant-in-Aid for Scientific Research and for Health and Labour Science Research Grants, Research on Advanced Medical Technology, H14-Toxico-007

REFERENCES

Alizadeh, A. A.; Eisen, M. B.; Davis, R. E.; Ma, C.; Lossos, I. S.; Rosenwald, A.; Boldrick, J. C.; Sabet, H.; Tran, T.; Yu, X.; Powell, J. I.; Yang, L.; Marti, G. E.; Moore, T.; Hudson, J. Jr.; Lu, L.; Lewis, D. B.; Tibshirani, R.; Sherlock, G.; Chan, W. C.; Greiner, T. C.; Weisenburger, D. D.; Armitage, J. O.; Warnke, R.; Levy, R.; Wilson, W.; Grever, M. R.; Byrd, J. C.; Botstein, D.; Brown, P. O. and Staudt, L. M. (2000) Distinct types of diffuse large B-cell lymphoma identified by gene expression profiling. *Nature* **403**, 503-511.

Al Moustafa, A. E.; Aloui-Jamali, M. A.; Batist, G.; Hernandez-Perez, M.; Serruya, C.; Alpert, L.; Black, M. J.; Sladek, R. and Foulkes, W. D. (2002) Identification of genes associated with head and neck carcinogenesis by cDNA microarray comparison between matched primary normal epithelial and squamous cell carcinoma cells. *Oncogene* **21**(17), 2634-2640.

Ando, T.; Suguro, M.; Hanai, T.; Kobayashi, T.; Honda, H. and Seto, M. (2002) Fuzzy neural network applied to gene expression profiling for predicting the prognosis of diffuse large B-cell lymphoma. *Jpn. J. Cancer Res.* **93**, 1207-1212.

Beer, D. G.; Kardia, S. L.; Huang, C. C.; Giordano, T. J.; Levin, A. M.; Misek, D. E.; Lin, L.; Chen, G.; Gharib, T. G.; Thomas, D. G.; Lizyness, M. L.; Kuick, R.; Hayasaka, S.; Taylor, J. M.; Iannettoni, M. D.; Orringer, M. B. and Hanash, S. (2002) Gene-expression profiles predict survival of patients with lung adenocarcinoma. *Nat. Med.* **8**, 816-824.

Bonenkamp, J. J.; Hermans, J.; Sasako, M. and van de Velde, C. J. (1999) Extended lymph-node dissection for gastric cancer. Dutch Gastric Cancer Group. *N. Engl. J. Med.* **340**, 908-914.

Brazma, A.; Hingamp, P.; Quackenbush, J.; Sherlock, G.; Spellman, P.; Stoeckert, C.; Aach, J.; Ansorge, W.; Ball, C. A.; Causton, H. C.; Gaasterland, T.; Glenisson, P.; Holstege, F. C.; Kim, I. F.; Markowitz, V.; Matese, J. C.; Parkinson, H.; Robinson, A.; Sarkans, U.; Schulze-Kremer, S.; Stewart, J.; Taylor, R.; Vilo, J. and Vingron, M. (2001) Minimum information about a microarray experiment (MIAME)-toward standards for microarray data. *Nat. Genet.* **29**, 365-371.

Chuaqui, R. F.; Bonner, R. F. ; Best, C. J.; Gillespie, J. W.; Flaig, M. J.; Hewitt, S. M.; Phillips, J. L.; Krizman, D. B.; Tangria, M. A.; Ahram, M.; Linehan, W. M.; Knezevic, V. and Emmert-Buck, M. R. (2002) Postanalysis follow-up and validation of microarray experiments. *Nat. Genet.* **32**(Suppl.), 509-514.

Churchill, G. A. (2002) Fundamentals of experimental design for cDNA microarrays. *Nat. Genet.* **32**(Suppl.), 490-495.

Cuschieri, A.; Weeden, S.; Fielding, J.; Bancewicz, J.; Craven, J.; Joypaul, V.; Sydes, M. and Fayers, P. (1999) Patient survival after D1 and D2 resections for gastric cancer: long-term results of the MRC randomized surgical trial. Surgical Co-operative Group. *Br. J. Cancer* **79**, 1522-1530.

Enard, W.; Khaitovich, P.; Klose, J.; Zollner, S.; Heissig, F.; Giavalisco, P.; Nieselt-Struwe, K.; Muchmore, E.; Varki, A.; Ravid, R.; Doxiadis, G. M.; Bontrop, R. E. and Paabo, S. (2002) Intra- and interspecific variation in primate gene expression patterns. *Science* **296**, 340-343.

Gruvberger, S.; Ringner, M.; Chen, Y.; Panavally, S.; Saal, L. H.; Borg, A.; Ferno, M.; Peterson, C. and Meltzer, P. S. (2001) Estrogen receptor status in breast cancer is associated with remarkably distinct gene expression patterns. *Cancer Res.* **61**, 5979-5984.

Hao, X.; Sun, B.; Hu, L.; Lahdesmaki, H.; Dunmire, V.; Feng, Y.; Zhang, S. W.; Wang, H.; Wu, C.; Wang, H.; Fuller, G. N.; Symmans, W. F.; Shmulevich, I. and Zhang, W. (2004) Differential gene and protein expression in primary breast malignancies and their lymph node metastases as revealed by combined cDNA microarray and tissue microarray analysis. *Cancer* **100**(6), 1110-1122.

Hasegawa, S.; Furukawa, Y.; Li, M.; Satoh, S.; Kato, T.; Watanabe, T.; Katagiri, T.; Tsunoda, T.; Yamaoka, Y. and Nakamura, Y. (2002) Genome-wide analysis of gene expression in intestinal-type gastric cancers using a complementary DNA microarray representing 23,040 genes. *Cancer Res.* **62**, 7012-7017.

International Lymphoma Study Group. (1997) A clinical evaluation of the International Lymphoma Study Group classification of non-Hodgkin's lymphoma. The Non-Hodgkin's Lymphoma Classification Project. *Blood* **89**, 3909-3918.

Jemal, A.; Thomas, A.; Murray, T. and Thun, M. (2002) Cancer statistics, 2002. *CA. Cancer J. Clin.* **52**, 23-47.

Kikuchi, T.; Daigo, Y.; Katagiri, T.; Tsunoda, T.; Okada, K.; Kakiuchi, S.; Zembutsu, H.; Furukawa, Y.; Kawamura, M.; Kobayashi, K.; Imai, K. and Nakamura, Y. (2003). Expression profiles of non-small cell lung cancers on cDNA microarrays: identification of genes for prediction of lymph-node metastasis and sensitivity to anti-cancer drugs. *Oncogene* **22**, 2192-2205.

Kopans, D. B. (2003) Gene-expression signatures in breast cancer. *N. Engl. J. Med.* **348**, 1715-1717.

Kunkler, I. H. (2003) Gene-expression signatures in breast cancer. *N. Engl. J. Med.* **348**, 1715-1717.

Moreau, Y.; Aerts, S.; De Moor, B.; De Strooper, B. and Dabrowski, M. (2003) Comparison and meta-analysis of microarray data: from the bench to the computer desk. *Trends Genet.* **19**, 570-577.

Mountain, C. F. (1997) Revisions in the International System For Staging Lung Cancer. *Chest* **111**, 1710-1717.

Mousses, S.; Bubendorf, L.; Wagner, U.; Hostetter, G.; Kononen, J.; Cornelison, R.; Goldberger, N.; Elkahoun, A. G.; Willi, N.; Koivisto, P.; Ferhle, W.; Raffeld, M.; Sauter, G. and Kallioniemi, O. P. (2002) Clinical validation of candidate genes associated with prostate cancer progression in the CWR22 model system using tissue microarrays. *Cancer Res.* **62**(5), 1256-1260.

Ohira, T.; Akutagawa, S.; Usuda, J.; Nakamura, T.; Hirano, T.; Tsuboi, M.; Nishio, K.; Taguchi, F.; Ikeda, N.; Nakamura, H.; Konaka, C.; Saijo, N. and Kato, H. (2002). Up-regulated gene expression of angiogenesis factors in post-chemotherapeutic lung cancer tissues determined by cDNA macroarray. *Oncol. Rep.* **9**, 723-728.

Oleksiak, M. F.; Churchill, G. A. and Crawford, D. L. (2002) Variation in gene expression within and among natural populations. *Nat. Genet.* **32**, 261-266.

Parkin, D. M. (2001) Global cancer statistics in the year 2000. *Lancet Oncol.* **2**, 533-543.

Perou, C. M.; Sorlie, T.; Eisen, M. B.; van de Rijn, M.; Jeffrey, S. S.; Rees, C. A.; Pollack, J. R.; Ross, D. T.; Johnsen, H.; Akslen, L. A.; Fluge, O.; Pergamenschikov, A.; Williams, C.; Zhu, S. X.; Lonning, P. E.; Borresen-Dale, A. L.; Brown, P. O. and Botstein, D. (2000) Molecular portraits of human breast tumors. *Nature* **406**, 747-752.

Popat, U.; Przepiork, D.; Champlin, R.; Pugh, W.; Amin, K.; Mehra, R.; Rodriguez, J.; Giralt, S.; Romaguera, J.; Rodriguez, A.; Preti, A.; Andersson, B.; Khouri, I.; Claxton, D.; de Lima, M.; Donato, M.; Anderlini, P.; Gajewski, J.; Cabanillas, F. and van Besien, K. (1998) High-dose chemotherapy for relapsed and refractory diffuse large B-cell lymphoma: mediastinal localization predicts for a favourable outcome. *J. Clin. Oncol.* **16**, 63-69.

Scagliotti, G. V. and Novello, S. (2003) The dream is almost over...don't worry, look ahead. *Lung Cancer* **40**, 187-190.

Slonim, D. K (2002) From patterns to pathways: gene expression data analysis comes of age. *Nature genetics* **32**(Suppl.), 502-550.

Schiller, J. H.; Harrington, D.; Belani, C. P.; Langer, C.; Sandler, A.; Krook, J.; Zhu, J. and Johnson, D. H. Eastern Cooperative Oncology Group. (2002) Comparison of four chemotherapy regimens for advanced non-small-cell lung cancer. *N. Engl. J. Med.* **346**, 92-98.

Shipp, M. A.; Ross, K. N.; Tamayo, P.; Weng, A. P.; Kutok, J. L.; Aguiar, R. C.; Gaasenbeek, M.; Angelo, M.; Reich, M.; Pinkus, G. S.; Ray, T. S.; Koval, M. A.; Last, K. W.; Norton, A.; Lister, T. A.; Mesirov, J.; Neuberg, D. S.; Lander, E. S.; Aster, J. C. and Golub, T. R. (2002) Diffuse large B-cell lymphoma outcome prediction by gene-expression profiling and supervised machine learning. *Nat. Med.* **8**, 68-74.

Simon, R.; Radmacher, M. D.; Dobbin, K. and McShane, L. M. (2003) Pitfalls in the use of DNA microarray data for diagnostic and prognostic classification. *J. Natl. Cancer Inst.* **95**, 14-18.

Sorlie, T.; Perou, C. M.; Tibshirani, R.; Aas, T.; Geisler, S.; Johnsen, H.; Hastie, T.; Eisen, M. B.; van de Rijn, M.; Jeffrey, S. S.; Thorsen, T.; Quist, H.; Matese, J. C.; Brown, P. O.; Botstein, D.; Eystein, Lonning. P. and Borresen-Dale, A. L. (2001) Gene expression patterns of breast carcinomas distinguish tumor subclasses with clinical implications. *Proc. Natl. Acad. Sci. USA* **98**, 10869-10874.

Stoeckert, C. J. Jr.; Causton, H. C. and Ball, C. A. (2002) Microarray databases: standards and ontologies. *Nat. Genet.* **32**(Suppl.), 469-473.

Suganuma, K.; Kubota, T.; Saikawa, Y.; Abe, S.; Otani, Y.; Furukawa, T.; Kumai, K.; Hasegawa, H.; Watanabe, M.; Kitajima, M.; Nakayama, H. and Okabe, H. (2003) Possible chemoresistance-related genes for gastric cancer detected by cDNA microarray. *Cancer Sci.* **94**, 355-359.

Tan, P. K.; Downey, T. J.; Spitznagel, E. L. Jr.; Xu, P.; Fu, D.; Dimitrov, D. S.; Lempicki, R. A.; Raaka, B. M. and Cam, M. C. (2003) Evaluation of gene expression measurements from commercial microarray platforms. *Nucleic Acids Res.* **31**, 5676-5684.

Tsunoda, T.; Koh, Y.; Koizumi, F.; Tsukiyama, S.; Ueda, H.; Taguchi, F.; Yamaue, H.; Saijo, N. and Nishio, K. (2003). Differential gene expression profiles and identification of the genes relevant to clinicopathologic factors in colorectal cancer selected by cDNA array method in combination with principal component analysis. *Int. J. Oncol.* **23**, 49-59.

Tusher, V. G.; Tibshirani, R. and Chu, G. (2001) Significance analysis of microarrays applied to the ionizing radiation response. *Proc. Natl. Acad. Sci. USA* **98**, 5116-5121.

van de Vijver, M. J.; He, Y. D.; van't Veer, L. J.; Dai, H.; Hart, A. A.; Voskuil, D. W.; Schreiber, G. J.; Peterse, J. L.; Roberts, C.; Marton, M. J.; Parrish, M.; Atsma, D.; Witteveen, A.; Glas, A.; Delahaye, L.; van der Velde, T.; Bartelink, H.; Rodenhuis, S.; Rutgers, E. T.; Friend, S. H. and Bernards, R. (2002) A gene-

expression signature as a predictor of survival in breast cancer. *N. Engl. J. Med.* **347**, 1999-2009.

van 't Veer, L. J.; Dai, H.; van de Vijver, M. J.; He, Y. D.; Hart, A. A.; Mao, M.; Peterse, H. L.; van der Kooy, K.; Marton, M. J.; Witteveen, A. T.; Schreiber, G. J.; Kerkhoven, R. M.; Roberts, C.; Linsley, P. S.; Bernards, R. and Friend, S. H. (2002) Gene expression profiling predicts clinical outcome of breast cancer. *Nature* **415**, 530-536.

Weiss, M. M.; Kuipers, E. J.; Postma, C.; Snijders, A. M.; Siccama, I.; Pinkel, D.; Westerga, J.; Meuwissen, S. G.; Albertson, D. G. and Meijer, G. A. (2003) Genomic profiling of gastric cancer predicts lymph node status and survival. *Oncogene* **22**, 1872-1879.

West, M.; Blanchette, C.; Dressman, H.; Huang, E.: Ishida, S.; Spang, R.; Zuzan, H.; Olson, J. A. Jr.; Marks, J. R. and Nevins, J. R. (2001) Predicting the clinical status of human breast cancer by using gene expression profiles. *Proc. Natl. Acad. Sci. USA* **98**, 11462-11467.

White, S. L.; Gharbi, S.; Bertani, M. F.; Chan, H. L.; Waterfield, M. D. and Timms, J. F. (2004) Cellular responses to ErbB-2 overexpression in human mammary luminal epithelial cells: comparison of mRNA and protein expression. *Br. J. Cancer* **90**, 173-181.

Received: May 12, 2004 Accepted: January 24, 2005

Element Array by Scanning X-ray Fluorescence Microscopy after *Cis*-Diamminedichloro-Platinum(II) Treatment

Mari Shimura,[1] Akira Saito,[4,8,9] Satoshi Matsuyama,[5] Takahiro Sakuma,[1] Yasuhito Terui,[3] Kazumasa Ueno,[5] Hirokatsu Yumoto,[5] Kazuto Yamauchi,[5] Kazuya Yamamura,[6] Hidekazu Mimura,[5] Yasuhisa Sano,[5] Makina Yabashi,[7] Kenji Tamasaku,[8] Kazuto Nishio,[2] Yoshinori Nishino,[8] Katsuyoshi Endo,[6] Kiyohiko Hatake,[3] Yuzo Mori,[6] Yukihito Ishizaka,[1] and Tetsuya Ishikawa[8]

[1]Department of Intractable Diseases, International Medical Center of Japan; [2]Pharmacology Division, National Cancer Center Research Institute; [3]Division of Clinical Chemotherapy, Cancer Chemotherapy Center, Japanese Foundation for Cancer Research, Tokyo, Japan; Departments of [4]Material and Life Science and [5]Precision Science and Technology, and [6]Research Center for Ultra-Precision Science and Technology, Graduate School of Engineering, Osaka University, Suita, Osaka, Japan; [7]SPring-8/Japan Synchrotron Radiation Research Institute and [8]SPring-8/Riken, Hyogo, Japan; and [9]Nanoscale Quantum Conductor Array Project, ICORP, Saitama, Japan

Abstract

Minerals are important for cellular functions, such as transcription and enzyme activity, and are also involved in the metabolism of anticancer chemotherapeutic compounds. Profiling of intracellular elements in individual cells could help in understanding the mechanism of drug resistance in tumors and possibly provide a new strategy of anticancer chemotherapy. Using a recently developed technique of scanning X-ray fluorescence microscopy (SXFM), we analyzed intracellular elements after treatment with *cis*-diamminedichloro-platinum(II) (CDDP), a platinum-based anticancer agent. The images obtained by SXFM (element array) revealed that the average Pt content of CDDP-resistant cells was 2.6 times less than that of sensitive cells, and the zinc content was inversely correlated with the intracellular Pt content. Data suggested that Zn-related detoxification is responsible for resistance to CDDP. Of Zn-related excretion factors, glutathione was highly correlated with the amount of Zn. The combined treatment of CDDP and a Zn(II) chelator resulted in the incorporation of thrice more Pt with the concomitant down-regulation of glutathione. We propose that the generation of an element array by SXFM opens up new avenues in cancer biology and treatment. (Cancer Res 2005; 65(12): 4998-5002)

Introduction

Cis-Diamminedichloro-platinum(II) (CDDP) is an effective anticancer agent, but tumor cells can become resistant after CDDP-based therapy (1). Detoxification of CDDP, an increase in DNA repair, and excretion of CDDP have been implicated as major factors contributing to CDDP resistance (1). Incorporated CDDP is excreted by several molecules, such as overexpressed P-glycoprotein (2), a zinc-related defense system that is regulated by increased intracellular glutathione (GSH; ref. 3), and the ATP-dependent glutathione S-conjugate export pump (GS-X pump), which plays a role in the vesicle-mediated excretion of GSH-CDDP conjugates from resistant cells (4). Recent reports suggest that minerals such as zinc (Zn) and copper (Cu), important for normal cellular functions (5), are involved in CDDP resistance (6, 7). The simultaneous monitoring of multiple numbers of cellular elements would be helpful in identifying the mechanism of drug resistance in a malignant cell. The recently developed technique of scanning X-ray fluorescence microscopy (SXFM; refs. 8, 9) has made it possible to detect elements of interest by a single measurement and give a profile of these elements at the single-cell level (termed an element array). To examine the efficacy of element array analysis, we analyzed elements before and after treatment with CDDP and compared the element profiles of CDDP-sensitive and CDDP-resistant cells. We showed that the Zn content has an inverse correlation with Pt incorporation owing to a positive linkage with glutathione (GSH), a Zn-dependent detoxification factor. The combined treatment with CDDP and *N,N,N,N*-tetrakis-(2-pyridylmethyl)-ethylenediamine (TPEN), a Zn (II)-chelator (10), increased Pt uptake with a concomitant reduction of intracellular GSH. We propose that the element array is a versatile method suitable for obtaining information about metals involved in drug metabolism and could contribute to a novel strategy for anticancer chemotherapy.

Materials and Methods

Element array analysis by scanning X-ray fluorescence microscopy. SXFM was set up at an undulator beamline, BL29XU, of the SPring-8 synchrotron radiation facility (11) by combining a Kirkpatrick-Baez–type X-ray focusing system (12, 13), an XY-scanning stage for sample mounting, and an energy-dispersive X-ray detector (SDD, Röntec, Co., Ltd.). Monochromatic X-rays at 15 keV for Pt *L*-line excitation were focused into a 1.5 μm (*H*) × 0.75 μm (*W*) spot with a measured flux of ~ 1×10^{11} photons/s. The focused X-rays simultaneously yielded the fluorescence of various chemical species in a small volume of sample cells, as shown in Fig. 1*A*. The fluorescence from each element was taken independently and did not overlap except for the Pt$L\alpha$ signal, which was contaminated by Zn$K\beta$ (Fig. 1*A*). This was corrected by subtraction, as described previously (8). In this study, we could also measure Pt$L\beta$ as a unique signal of Pt (Fig. 1*A*). After counts were collected for 4.0 to 8.5 seconds at each pixel of scanning, the detected counts were normalized by incident beam intensity. In addition to the mapping images, an elemental concentration per single cell was calculated from the integrated elemental intensity over the whole mapping image.[10]

Requests for reprints: Yukihito Ishizaka, Department of Intractable Diseases, International Medical Center of Japan, 1-21-1 Toyama, Shinjuku-ku, 162-8655 Tokyo, Japan. Phone/Fax: 81-3-5272-7527; E-mail: zakay@ri.imcj.go.jp.

[10] A. Saito et al., manuscript in preparation.

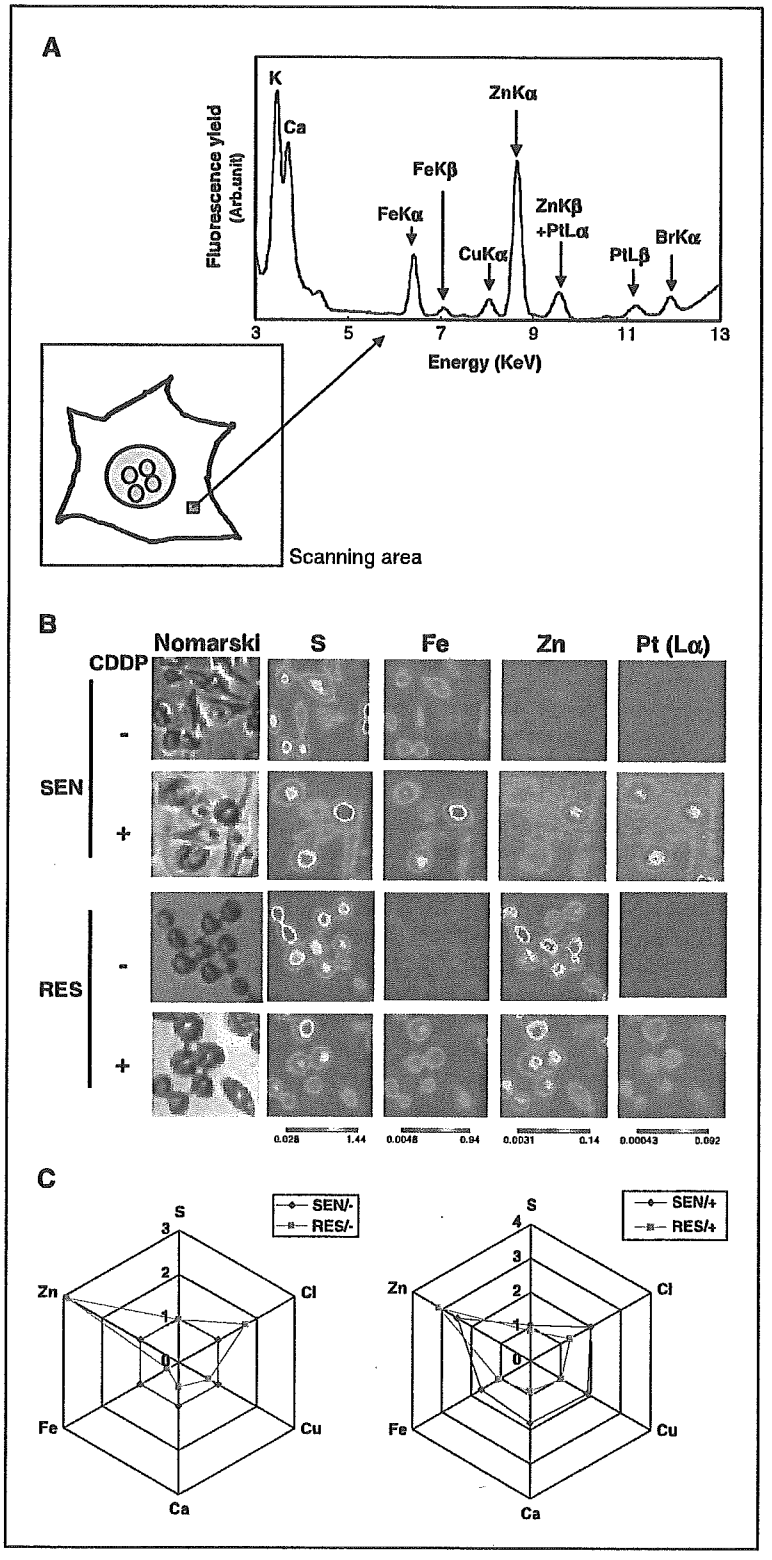

Figure 1. Element array by SXFM. *A,* scheme of imaging cellular elements by SXFM. Coherent X-rays are focused on each area (*pixel*), and the X-ray fluorescence from each element is detected. Each pixel gives an elemental spectrum, as shown in the right panel, and an integrated intensity of the individual element was mapped to the corresponding area of analyzed cells. *B,* SXFM analysis after CDDP treatment. Cell morphologies obtained by Nomarski are shown at ×100 magnification (*left*). Each field of view is equivalent to an area of 70 × 70 μm. Representative results are shown. Brighter colors indicate a higher signal intensity of each element. Results are shown for PC/SEN (*top*) and PC/RES cells (*bottom*). Note the high intensity of Pt*Lα* in PC/SEN cells after CDDP treatment (*second panel of the Pt column*) and the higher signal intensity of Zn in PC/RES cells compared with that of PC/SEN cells. *C,* element array based on SXFM analysis. The mean signal intensity of each element obtained by SXFM analysis was calculated, and the fold increase of elements in PC/RES cells (*red*) was depicted by using the intensity in PC/SEN cells (*blue*) as a standard (*left*). A part of analyzed elements is shown. The fold increase of elements in PC/SEN (*blue*) and PC/RES cells (*red*) after CDDP treatment was also shown by using the intensity in PC/SEN before CDDP treatment as a standard (*right*).

Chemicals and biochemical assays. TPEN (Sigma, St. Louis, MO; ref. 10), GSH (Calbiochem, La Jolla, CA), and CDDP (Daiichi Kagaku, Tokyo, Japan) were purchased. A GSH colorimetric assay kit (Calbiochem) and a BCA protein assay kit (Bio-Rad, Hercules, CA) were used for measuring intracellular GSH. About 3×10^5 to 4×10^5 cells were subjected to GSH measurement, and the data were normalized by cell number.

Cell lines. PC-9 cells (PC/SEN) and PC-9 cells resistant to CDDP (PC/RES), originally derived from a lung carcinoma cell line (14), were

maintained in DMEM (Nissui, Co., Tokyo, Japan) supplemented with 10% FCS (Sigma). The viability of PC/SEN cultured for 72 hours in the presence of 1 μmol/L CDDP was 40%, whereas that of PC/RES was ~90%. In this study, each cell line when treated with 1 μmol/L CDDP for 24 hours showed >85% viability.

Colony formation. After treatment, aliquots of PC/SEN and PC/RES were plated into culture dishes or soft agar, and the numbers of cell aggregates consisting of >50 cells were counted. Each number was normalized by plating efficiency, and the mean and SD of the number of formed colonies were calculated.

Sample preparation. Cells were plated on a silicon nitride base (NTT Advanced Technology, Tokyo, Japan) 1 day before the experiment. After incubation for 24 hours in the presence of 1 μmol/L CDDP, the cells were washed with PBS, fixed in 2% paraformaldehyde in PBS for 10 minutes at room temperature, and incubated in cold 70% ethanol for 30 minutes. The cells were then placed in a 1:3 solution of glacial acetic acid and methanol for 10 minutes, washed with 70% alcohol, and dried overnight at room temperature.

Measurement of cellular platinum and zinc. To measure Pt and Zn, ~5 × 10^6 cells were subjected to inductively coupled plasma mass spectroscopy (ICP-MS; Toray Research Center, Shiga, Japan; ref. 15).

Statistical analysis. The Pearson product-moment correlation coefficient and Student's *t* test were used to evaluate statistical significance (16).

Results and Discussion

Incorporation of platinum and element array after *cis*-diamminedichloro-platinum(II) treatment. We analyzed intracellular elements by SXFM after CDDP treatment (Fig. 1*A*). At 12 hours after treatment with 1 μmol/L CDDP, the level of Pt was increased in PC/SEN cells, whereas little increase in the Pt level was seen in PC/RES cells (Fig. 1*B*). The intensity of Pt in PC/RES cells was 2.6-fold less than that in PC/SEN cells, as confirmed by the results of ICP-MS, which indicated that the amount of Pt in PC/RES cells (5.5 fg/cell) was 3.6-fold less than that in PC/SEN cells (19.7 fg/cell). Therefore, the decreased accumulation of CDDP is likely to be responsible for resistance in PC/RES cells.

Based on the mean signal intensity obtained by SXFM, element array analysis was carried out (Fig. 1*C*). The element profile

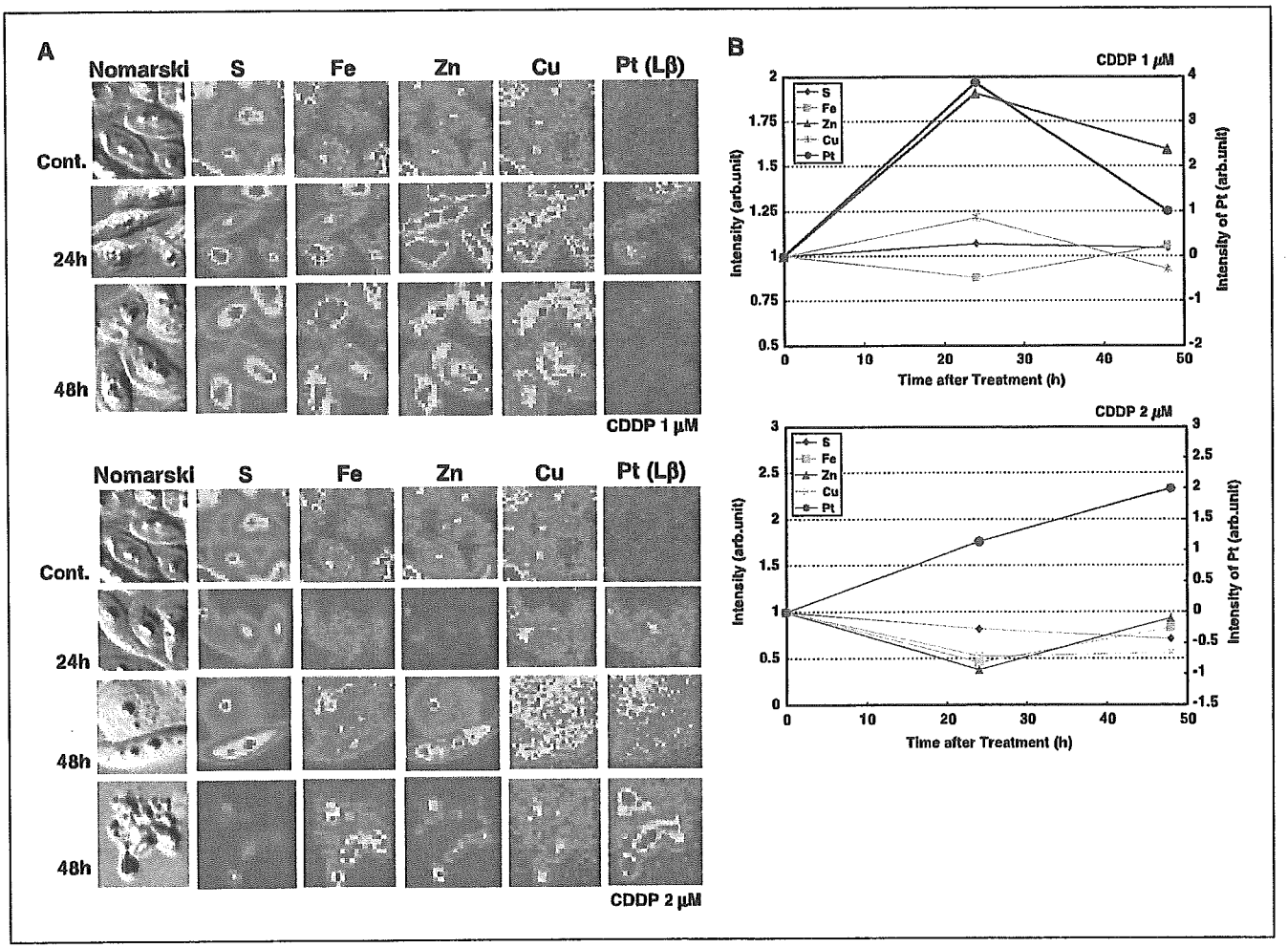

Figure 2. Chronological changes in elements after CDDP treatment. *A*, detection of elements in CDDP-treated PC/SEN cells. From the left, Nomarski images, signals of S, Fe, Zn, Cu, and Pt are shown. Top and bottom sets of panels show cells treated with 1 and 2 μmol/L CDDP, respectively. In each set of panels, control cells (*top*) and cells treated with CDDP for 24 hours (*middle*) and 48 hours (*bottom*) are shown. In this experiment, the signals of Pt*Lβ* were measured instead of Pt*Lα* (see Materials and Methods). The lowest panels show an apoptotic cell after 48 hours. *B*, summarized results of chronological changes of elements. The results after treatment with 1 μmol/L (*top*) and 2 μmol/L CDDP (*bottom*) are shown. The mean signal intensity was calculated from the results partly shown in (*A*). Among the cellular elements, Zn was most influenced by both 1 and 2 μmol/L CDDP treatment and had an inverse correlation with Pt content.

03

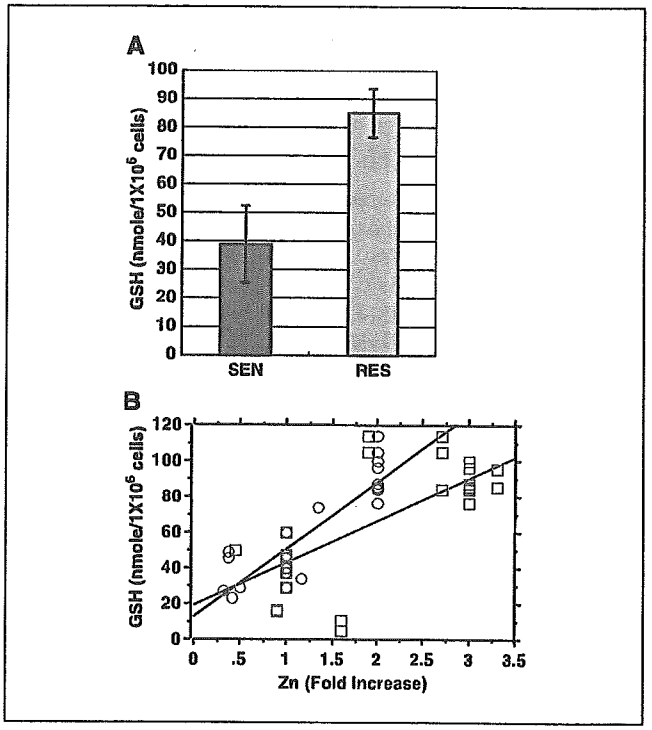

Figure 3. Cellular Zn content and GSH. *A*, basal level of intracellular GSH. The intracellular GSH levels in PC/SEN (*black*) and PC/RES cells (*gray*) were measured. GSH was significantly higher in PC/RES than in PC/SEN cells (*t* test, $P < 0.05$). *B*, correlation between Zn and intracellular GSH. A scatter diagram for Pearson product-moment correlation coefficient is depicted. Zn, measured by SXFM (*red squares*, $n = 27$) and by ICP-MS (*green circles*, $n = 29$), was plotted against intracellular GSH. Scattered values were based on data from both PC/SEN and PC/RES cells. The correlation coefficient r was calculated, and the statistical significance was determined ($P < 0.05$).

facilitates the identification of the elements related to the mechanism of drug resistance to CDDP. First, we noticed that the Zn content of untreated PC/RES cells was ~3-fold of that in PC/SEN cells (Fig. 1*C*, *left*). The difference in the Zn contents of these cells was confirmed by ICP-MS analysis (105 fg/cell for PC/SEN cells and 189 fg/cell for PC/RES cells, respectively). When 1 μmol/L CDDP was used for treatment, constitutive high Zn was observed in PC/RES (Fig. 1*C*, *right*). In PC/SEN cells, the amounts of all the elements were slightly increased, but the amount of Zn was increased most markedly.

We then analyzed the chronological changes in the levels of elements in PC/SEN cells following CDDP treatment. Representative results for S, Fe, Zn, Cu, and Pt are shown in Fig. 2*A*. Pt was clearly observed at 24 hours after treatment with 1 or 2 μmol/L CDDP (Fig. 2*A*). It was, however, barely detectable at 48 hours after the cells were treated with 1 μmol/L CDDP (Fig. 2*A*, *top*), suggesting that the cells excreted CDDP. In contrast, the cellular content of Pt gradually increased after treatment with 2 μmol/L CDDP (Fig. 2*A*, *bottom*), and apoptotic cells with high levels of incorporated CDDP were observed after 48 hours (Fig. 2*A*, *bottom*).

The element profile was plotted against the time after treatment with CDDP (Fig. 2*B*). When the cells were treated with 1 μmol/L CDDP, the Zn content increased remarkably and reached a peak at 24 hours (Fig. 2*B*, *top*, *red line*). In these cells, the Pt content was reduced after 48 hours. When the cells were treated with 2 μmol/L CDDP, the Zn content decreased within 24 hours (Fig. 2*B*, *bottom*), and the Pt content increased within 48 hours. In this analysis, Cu did not show significant changes. The results imply that the intracellular Zn content has an inverse correlation with the incorporated Pt content.

Cellular zinc and zinc-related detoxification. We studied Zn-related detoxification factors, such as metallothioneins (17), GSH (18), and the GSH-coupled excretory pump GS-X (4), and we observed that intracellular GSH was high in PC/RES cells (Fig. 3*A*). We then examined the possible correlation between the intracellular Zn content and GSH. As shown in Fig. 3*B*, the GSH levels showed a significant correlation with the levels of Zn detected by both ICP-MS and SXFM (Pearson product-moment correlation coefficient $r = 0.794$, $P < 0.05$ and $r = 0.533$, $P < 0.05$, respectively). The levels of Zn detected by SXFM may have less correlation with GSH than do the levels detected by ICP-MS because SXFM analyzed Zn in a small number of cells, whereas the analyses of GSH using ICP-MS were carried out on $>10^5$ cells.

Effects of zinc depletion and *cis*-diamminedichloroplatinum(II) uptake. To examine ways of increasing the sensitivity of PC/RES cells to CDDP, we used the Zn(II) chelator TPEN, as it was thought that CDDP uptake would increase when the GSH level was down-regulated by decreased Zn. Consistent with this hypothesis, treatment with 7.5 μmol/L of TPEN decreased cellular Zn to ~40 fg/cell at 30 hours after treatment in PC/SEN cells (Fig. 4*A*, *left*, *solid line*). The decrease seen in PC/RES cells owing to TPEN treatment was more rapid, with the Zn concentration being reduced to ~40 fg/cell within 7 hours (Fig. 4*A*, *left*, *dashed line*). The intracellular GSH also decreased with the reduction in intracellular Zn (Fig. 4*A*, *right*, *dashed line*).

To determine the effects of TPEN on the growth of PC/RES cells, the cells were pulse-treated for 2 hours with TPEN for 5 consecutive days and the growth was examined. Although treatment with 1 μmol/L CDDP did not induce apparent morphologic changes (Fig. 4*B*, *bottom*, *left*), the combined treatment with TPEN and CDDP caused prominent changes (Fig. 4*B*, *bottom*, *right*). A colony formation assay clearly showed that the combination of CDDP and TPEN, as well as single TPEN treatment, significantly impaired the growth of PC/RES cells (Fig. 4*C*). Consistent with these changes, ICP-MS indicated that the intracellular Pt content increased 3.5-fold after the combined treatment (from 0.38 to 1.35 fg/cell with TPEN treatment). It is important to note that the same dose of TPEN did not attenuate the growth of PC/SEN cells (Fig. 4*C*). These data indicate that the GSH level seems to be critical for resistance in PC/RES cells, consistent with previous reports that CDDP-resistant cells have high levels of GSH and that a decrease in GSH results in loss of resistance (3, 19). Our data also suggest that the high GSH content was maintained by the effects of Zn in PC/RES cells. Overall, our trial treatment with combined TPEN and CDDP suggests that this combination would be effective in eliminating tumors even if they include a CDDP-resistant population of cells with high Zn content.

We showed the use of element array analysis by SXFM to examine a mechanism of CDDP resistance. Based on element profiles, we successfully overcame CDDP resistance in PC/RES cells by using a Zn chelator that down-regulated the GSH level. Although it has been reported that Cu is a necessary factor for CDDP incorporation (7), the present work revealed that Cu was not involved in PC/RES cells. It is tempting to speculate that drug resistance is generated by various elements, and we propose that an element array can contribute to better understanding of cancer biology as well as other fields of medical science.

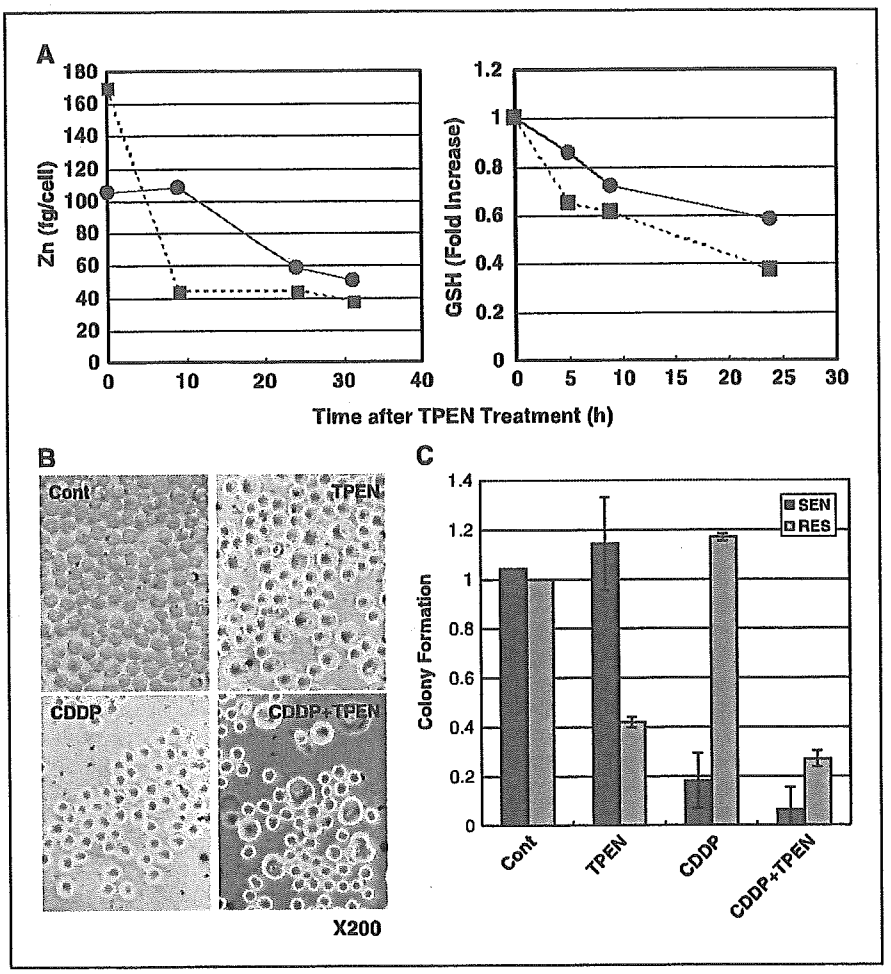

Figure 4. Cellular Zn content and Pt uptake with TPEN. *A*, TPEN-induced depletion of cellular Zn and down-regulation of GSH. TPEN (7.5 μmol/L) was added to the culture medium for the indicated time periods, and cellular Zn was measured by ICP-MS (*left*). Intracellular GSH content was also monitored (*right*). The Zn contents in PC/SEN (*solid lines*) and PC/RES cells (*dashed lines*) are shown. *B*, morphologic changes after pulse treatment with TPEN and CDDP. The morphologies of untreated PC/RES cells (*top*, *left*) and of cells treated with TPEN (*top*, *right*), CDDP (*bottom*, *left*), and CDDP plus TPEN (*bottom*, *right*) are shown. The cells were exposed to 1.0 μmol/L CDDP with or without 7.5 μmol/L TPEN for 2 hours, and then the medium was replaced with fresh medium. Pulse treatment was carried out for 5 consecutive days. Magnification, ×200. Note that large cells are observed after treatment with TPEN alone, and larger cells with irregular shape are observed following the combination treatment. The data showed that TPEN caused cellular accumulation at G_2-M phase with mitotic failure (data not shown). *C*, colony formation after pulse treatment with CDDP with or without TPEN. After pulse treatment for 5 consecutive days, as described in (*B*), the cells were plated in soft agar and the colony formation assay was done. The means and SDs of colony numbers of PC/SEN (*black columns*) and PC/RES cells (*gray columns*) are shown. The experiments were carried out in triplicate.

Acknowledgments

Received 2/3/2005; accepted 4/20/2005.

Grant support: Grant-in-aid for scientific research from the Ministry of Health, Labor, and Welfare of Japan and grant-in-aid for Center of Excellence Research (grant 08CE2004) from the Ministry of Education, Sports, Culture, Science, and Technology of Japan. The usage of BL29XU of the SPring-8 was supported by RIKEN.

The costs of publication of this article were defrayed in part by the payment of page charges. This article must therefore be hereby marked *advertisement* in accordance with 18 U.S.C. Section 1734 solely to indicate this fact.

We thank Harumi Shibata and Yasunori Suzuki for technical assistance.

References

1. Boulikas T, Vougiouka M. Cisplatin and platinum drugs at the molecular level. Oncol Rep 2003;10:1663–82.
2. Kuo TH, Liu FY, Chuang CY, Wu HS, Wang JJ, Kao A. To predict response chemotherapy using ^{99m}technetium tetrofosmin chest images in patients with untreated small cell lung cancer and compare with p-glycoprotein, multidrug resistance related protein-1, and lung resistance-related protein expression. Nucl Med Biol 2003;30:627–32.
3. Godwin AK, Meister A, O'Dwyer PJ, Huang CS, Hamilton TC, Anderson ME. High resistance to cisplatin in human ovarian cancer cell lines is associated with marked increase of glutathione synthesis. Proc Natl Acad Sci U S A 1992;89:3070–4.
4. Ishikawa T, Wright CD, Ishizuka H. GS-X pump is functionally overexpressed in *cis*-diamminedichloroplatinum (II)-resistant human leukemia HL-60 cells and down-regulated by cell differentiation. J Biol Chem 1994;269:29085–93.
5. Mayes PA, Nutrition. In: Murray RK, Granner DK, Mayers PA, Rodwell VW, editors. Harper's biochemistry. Chapter 54. 25th ed. New York: McGraw-Hill; 2000. p. 653–61.
6. Koropatnick J, Pearson J. Zinc treatment, metallothionein expression, and resistance to cisplatin in mouse melanoma cells. Somat Cell Mol Genet 1990;16:529–37.
7. Katano K, Kondo A, Safaei R, et al. Acquisition of resistance to cisplatin is accompanied by changes in the cellular pharmacology of copper. Cancer Res 2002;62:6559–65.
8. Ilinski P, Lai B, Cai Z, et al. The direct mapping of the uptake of platinum anticancer agents in individual human ovarian adenocarcinoma cells using a hard X-ray microprobe. Cancer Res 2003;63:1776–9.
9. Hall MD, Dillon CT, Zhang M, et al. The cellular distribution and oxidation state of platinum(II) and platinum(IV) antitumor complexes in cancer cells. J Biol Inorg Chem 2003;8:726–32.
10. Parat M-O, Richard M-J, Meplan C, Favir A, Béani J-C. Impairment of cultured cell proliferation and metallothionein expression by metal chelator *NNN' N'*-tetrakis-(2-pyridylmethyl)ethylene diamine. Biol Trace Elem Res 1999;70:51–68.
11. Miao J, Hodgson KO, Ishikawa T, Larabell CA, LeGros MA, Nishino Y. Imaging whole *Escherichia coli* bacteria by using single-particle X-ray diffraction. Proc Natl Acad Sci U S A 2003;100:110–2.
12. Kirkpatrick P, Baez AV. Formation of optical images by X-rays. J Opt Soc Am 1948;38:766–74.
13. Yamauchi K, Yamamura K, Mimura H, et al. Two-dimensional submicron focusing of hard X-rays by two elliptical mirrors fabricated by plasma chemical vaporization machining and elastic emission machining. Jpn J Appl Phys 2003;42:7129–34.
14. Kawamura-Akiyama Y, Kusaba H, Kanzawa F, Tamura T, Saijo N, Nishio K. Non-cross resistance of ZD0473 in acquired cisplatin-resistant lung cancer cell lines. Lung Cancer 2002;38:43–50.
15. Richarz AN, Wolf C, Bratter P. Determination of protein-bound trace elements in human cell cytosols of different organs and different pathological states. Analyst 2003;128:640–5.
16. Glantz SA. How to test for trends. In: Glantz SA, editor. Primer of biostatistics. Chapter 8. 2nd ed. New York: McGraw-Hill; 1987. p. 191–244.
17. Jourdan E, Jeanne RM, Régine S, Pascale G. Zinc-metallothinein genoprotective effect is independent of the glutathione depletion in HaCaT keratinocytes after solar light irradiation. J Cell Biochem 2004;92:631–40.
18. Parat M-O, Richard M-J, Béani J-C, Favier A. Involvement of zinc in intracellular oxidant/antioxidant balance. Biol Trace Elem Res 1997;60:187–204.
19. Hamaguchi K, Godwin AK, Yakushiji M, O'Dwyer PJ, Ozols RH, Hamilton TC. Cross-resistance to diverse drugs is associated with primary cisplatin resistance in ovarian cancer cell lines. Cancer Res 1993;53:5225–32.

Development and biological analysis of peritoneal metastasis mouse models for human scirrhous stomach cancer

Kazuyoshi Yanagihara,[1,6] Misato Takigahira,[1] Hiromi Tanaka,[1] Teruo Komatsu,[1] Hisao Fukumoto,[5] Fumiaki Koizumi,[5] Kazuto Nishio,[2] Takahiro Ochiya,[3] Yoshinori Ino[4] and Setsuo Hirohashi[4]

[1]Central Animal Laboratory; [2]Pharmacology Division; [3]Section for Studies on Metastasis; [4]Pathology Division, National Cancer Center Research Institute; and [5]Shien-Lab Medical Oncology Department, National Cancer Center Hospital, 5-1-1 Tsukiji, Chuo-ku, Tokyo 104-0045, Japan

(Received February 23, 2005/Accepted March 26, 2005/Online publication June 15, 2005)

The number of published studies on peritoneal dissemination of scirrhous gastric carcinoma is very small as a result of the unavailability of highly reproducible animal models. Orthotopic implantation of HSC-44PE and HSC-58 (scirrhous gastric carcinoma-derived cell lines) cells into nude mice led to dissemination of the tumor cells to the greater omentum, mesenterium, peritoneum and so on, and caused ascites in a small number of animals. Cycles of isolation of the ascitic tumor cells and orthotopic inoculation of these cells were repeated in turn to animals. This was to isolate highly metastatic cell lines with a strong capability of inducing the formation of ascites (44As3 from HSC-44PE; 58As1 and 58As9 from HSC-58). All three cell lines induced tumor formation at the site of orthotopic injection, and caused fatal cancerous peritonitis and bloody ascites in 90–100% of the animals approximately 3–5 weeks after the inoculation. When the parent cells were implanted, the animals became moribund in approximately 12–18 weeks, however, none of the animals developed ascites. Complementary DNA microarray and immunohistochemical analyses revealed differences in the expression levels of genes coding for the matrix proteinase, cell adhesion, motility, angiogenesis and proliferation between the highly metastatic- and parent-cell lines. The usefulness of this model for the evaluation of drugs was assessed by analyzing the stability of the metastatic potential of the cells and the reproducibility. Animals intravenously treated with CPT-11 and GEM showed suppressed tumor growth and significantly prolonged survival. The metastatic cell lines and the *in vivo* model established in the present study are expected to serve as a model of cancerous peritonitis developing from primary lesions, and as a useful means of clarifying the pathophysiology of peritoneal dissemination of scirrhous gastric carcinoma and the development of drugs for its treatment. (*Cancer Sci* 2005; 96: 323–332)

Although therapeutic results for gastric cancer have improved recently, the prognosis of patients with scirrhous gastric carcinoma still remains very poor. Scirrhous gastric carcinoma (diffusely infiltrative carcinoma or Borrmann's type-IV carcinoma, or the linitis plastica-type carcinoma) is characterized macroscopically by rigid thickening of the involved region of the gastric wall, causing it to assume a plate-like appearance, rather than by a well-defined mass.[1] Histopathologically, scirrhous cancer cells do not form glands, but cause diffuse infiltration of a broad region of the gastric wall, resulting in fibrous-like thickening of the gastric wall.[2,3] Because of such pathological features, early clinical diagnosis of scirrhous gastric carcinoma is difficult. By the time the diagnosis is made, peritoneal dissemination or distant metastasis to lymph nodes has already occurred in many cases. Peritoneal dissemination occurs frequently even after radical surgery, and is the cause of death in many patients.[4,5] Thus, peritoneal dissemination, a frequent form of recurrence and metastasis of scirrhous gastric carcinoma, serves as a major factor determining the prognosis of patients with scirrhous gastric carcinoma. To date, however, the mechanism of peritoneal dissemination in this type of cancer has not yet been fully elucidated.

Several theories have been proposed to explain the mechanism of peritoneal dissemination in human gastric cancer; it has been suggested that the cancer cells are detached from the primary lesions and freed into the peritoneal cavity, to colonize the peritoneum and induce cancerous peritonitis. However, most of the proposed theories remain speculations, and are seldom based on adequate evidence.[6–8] It cannot be overemphasized therefore that animal models of this condition are urgently needed to pursue studies on its pathophysiology. Some investigators have reported on a model of this condition established by direct inoculation of cultured gastric cancer cells into the peritoneal cavity.[9,10] It is difficult, however, to view this model as faithfully reflecting the characteristics of cancerous peritonitis observed in clinical cases. In the past, it was considered difficult to reliably establish a model of peritoneal dissemination developing from the primary lesions. Under these circumstances, we established seven cultured cell lines derived from human scirrhous gastric carcinoma and analyzed their characteristics.[11–14] Of these cell lines, the HSC-44PE and HSC-58 cells were found to show spontaneous metastasis to lymph nodes and lungs following s.c. implantation in nude mice.[14] Then, to isolate cell lines with a high metastatic potential, we performed repetitive s.c. inoculation of these cell lines and isolated sublines that tended to metastasize to lymph nodes. When these sublines were implanted orthotopically, a small number of animals showed massive bloody ascites. This phenomenon resembled the cancerous peritonitis seen in clinical cases and suggested a high possibility of establishing a reproducible mouse model of peritoneal dissemination.

In the present paper, we shall report on an analysis of the characteristics of tumor cell lines that often cause ascites (cell lines with a high potential for peritoneal dissemination) isolated by repeated orthotopic implantation of HSC-44PE and HSC-58 cells. The paper will also describe the results of cDNA microarray and immunohistochemical analyses of these cell lines as the first step towards clarifying the molecular mechanism of development of peritoneal metastasis in gastric cancer. In addition, the usefulness of these cell lines as a model for drug evaluation will also be discussed.

[6]To whom correspondence should be addressed. E-mail: kyanagih@gan2.res.ncc.go.jp
Abbreviations: cDNA, complementary DNA; CPT-11, camptothecin; GEM, gemcitabine; s.c., subcutaneously; i.p., intraperitoneally; i.v., intravenously.

 doi: 10.1111/j.1349-7006.2005.00054.x

Materials and Methods

Cell lines and culture. HSC-39, HSC-44PE and HSC-58 and cell lines established from human scirrhous gastric carcinomas have been reported previously.[11,14] The cell lines were maintained in RPMI1640 medium (Immuno-Biological Laboratories (IBL), Takasaki, Japan) supplemented with 10% FCS (Sigma Chemical, St. Louis, MO, USA), 100 IU/mL penicillin G sodium and 100 μg/mL streptomycin sulfate (IBL) in a 5% CO_2 and 95% air atmosphere at 37°C. The cells were passaged and expanded by trypsinization (0.05% trypsin and 0.02% EDTA; IBL), followed by replating every 5–7 days. All the cell lines were routinely tested for Mycoplasma by the Central Institute for Experimental Animals (Kawasaki, Japan), and no contamination was detected. For injection into mice, cells in log-phase growth were harvested by trypsinization and washed with serum-free RPMI1640 medium.

Animal experimentation. The animal experimental protocols were approved by the Committee for Ethics of Animal Experimentation, and the experiments were conducted in accordance with the Guidelines for Animal Experiments in the National Cancer Center. The mice were purchased from CLEA Japan (Tokyo, Japan) and maintained under specific pathogen-free conditions. They were provided with sterile food and water and housed in cages. The ambient light was controlled to provide regular 12-h light and 12-h darkness cycles.

Establishment of cell lines with a strong potential for inducing the formation of peritoneal metastasis. HSC-44PE and HSC-58 cell lines were inoculated by the orthotopic implantation technique into BALB/c nude mice. At appropriate intervals, or when moribund, the mice were sacrificed and the ascitic tumor cells were harvested aseptically. The cell suspensions were then cultured *in vitro*. The same procedure was repeated using both cell lines, and cell lines with a high potential for inducing the formation of peritoneal metastasis were established after 12 cycles of stepwise selection. Each resultant cell line after *in vitro* passages 5–10 was used for experiments.

Orthotopic implantation. Six-week-old female BALB/c nude mice were anesthetized by i.p. injection of 2.2.2-tribromoethanol (Aldrich Chemical, Milwaukee, WI, USA) at the dose of 0.28 mg/g bodyweight. Then, after making a small median abdominal incision in the mice under anesthesia, 2×10^6 cells in 0.05-mL volume of RPMI medium were inoculated into the middle wall of the greater curvature of the glandular portion of the stomach using a 30-gauge needle (Nipro, Tokyo, Japan). The stomach was then returned into the peritoneal cavity, and the abdominal wall and skin were closed with an AUTOCLIP applier (Becton-Dickinson, Sparks, MD, USA). The mice were killed 200 days after the tumor cell inoculation or when moribund, and peritoneal dissemination was evaluated by counting the number of tumor nodules in the mesenterium. The body organs were examined for metastasis, and various tissues were processed for histological examination.

Evaluation of the growth rate and metastatic potential of the cell lines. The tumorigenicity and spontaneous-metastatic potential of the cell lines were tested by s.c. injection of $0.5–1 \times 10^7$ cells suspended in 0.2 mL of RPMI1640 medium into 6-week-old female BALB/c nude mice. All the mice were numbered, housed separately, and examined twice weekly for tumor development. The tumor mass was measured in two dimensions with calipers, and the tumor volume was calculated according to the equation $(l \times w^2)/2$ (l = length, w = width). At appropriate intervals or when moribund, the mice were killed, and various organs and tissues were examined for metastasis and processed for histological examination as described.[11]

Therapeutic studies with CPT-11 and GEM. Orthotopic implantation of 2×10^6 44As3 or 58As1 cells was conducted in 6-week-old female BALB/c mice (Day 0). The experimental mice were divided into a control group that received vehicle alone (saline), and experimental groups that received i.v. inoculation of different doses of the drugs (50–200 mg/kg/mouse). On Days 3, 7 and 11, tumor-bearing mice received an i.v. injection of 7-Ethyl-10-[4-(1-piperidino)-1-piperidino] carboxycamptothecin (CPT-11). CPT-11 was purchased from Yakult Honsha (Tokyo, Japan) and dissolved in saline before being injected i.v. Gemcitabine (gemcitabine hydrochloride), chemically characterized as (+)-2′-deoxy-2′, 2′-difluorocytidine monohydrochloride, was purchased from Eli Lilly Japan (Kobe, Japan). The mice were administered i.v. inoculations of GEM on days 3, 7, 10, 14, 17, and 21. Seven mice from each group were killed when moribund, or on Day 70.

Statistical analysis. All the data were expressed as the mean ± SE, and analyzed using the unpaired t-test and a P-value of less than 0.001 was considered to denote statistical significance.

RT-PCR analysis. Total RNA was extracted using the ISOGEN/ISOGEN-LS Poly (A) + Isolation Pack (Nippon Gene, Tokyo, Japan), in accordance with the supplier's protocol. After reverse transcription using 1 μg total RNA with an oligo (dT) primer, the whole mixture was used for PCR detecting human and murine β actin. The primers used were as follows; human β actin forward primer, GGAAATCGTGCGTGACATT; reverse primer, CATCTGCTGGAAGGTGGACAG; murine β actin forward primer, GAAATCGTGCGTGACATCAAA; reverse primer, TACTGGTGCTAGGAGCCA. PCR was performed using an RNA PCR kit (Applied Biosystems, Foster City, CA, USA), under the following conditions; initial denaturation at 95°C for 2 min, 35 cycles of amplification (denaturation at 95°C for 60 s and annealing at 60°C for 60 s), and extension at 72°C for 7 min. The PCR products were electrophoresed on 2% agarose gel, and stained with ethidium bromide.

Gene expression profiling by cDNA microarray analysis. 5 μg total RNA was amplified using an *in vitro* transcription reaction.[15] The amplified RNA (6 μg) was reverse-transcribed using random hexamers and aminoallyl-dUTP. The synthesized cDNA was labeled by allowing it to react with a dye (NHS-ester Cy3 or Cy5, Amersham Biosciences, Buckinghamshire, UK).[16] The labeled cDNA was applied to the DNA microarray (Human IA; Agilent Technologies, Palo Alto, CA, USA) and hybridized at 65°C for 17 h. After washing, the microarray was scanned on a scanner (Agilent, G2565BA) and the image was analyzed using a Feature Extraction software (Agilent). The signal intensity of each spot was calibrated by subtraction from the intensity of the negative control. Global normalization methods were used for identification of the differentially expressed genes in each microarray experiment.

Immunohistochemical Analysis. Mouse antibodies against human Cathepsin L (C2970) and MMP-1 (M6427: Sigma-Aldrich, St. Louis, MO, USA), human VEGF (JH121: Laboratory Vision, Fremont, CA, USA), human EGER (31G7: Zymed Laboratory, San Francisco, CA, USA) and human Smad4 (B-8; Santa Cruz Biotechnology, Santa Cruz, CA, USA) were used for this study. The other antibodies used have been described in a previous study.[14] Immunohistochemical staining was carried out as described previously.[8] The staining was repeated to check for possible technical errors, but the results were consistent. Scores for the expression of various genes were assigned semiquantitatively according to the percentage of the cells stained and the staining intensity.

Results

Establishment of the highly metastatic cell lines. Following s.c. inoculation, 20–40% of the HSC-44PE and HSC-58 cells (cultured scirrhous gastric carcinoma cells) metastasized spontaneously to the regional lymph nodes and lungs. When the subclones isolated by repeated s.c. injection of these cells were implanted orthotopically, they spread to the greater omentum,

 doi: 10.1111/j.1349-7006.2005.00054.x

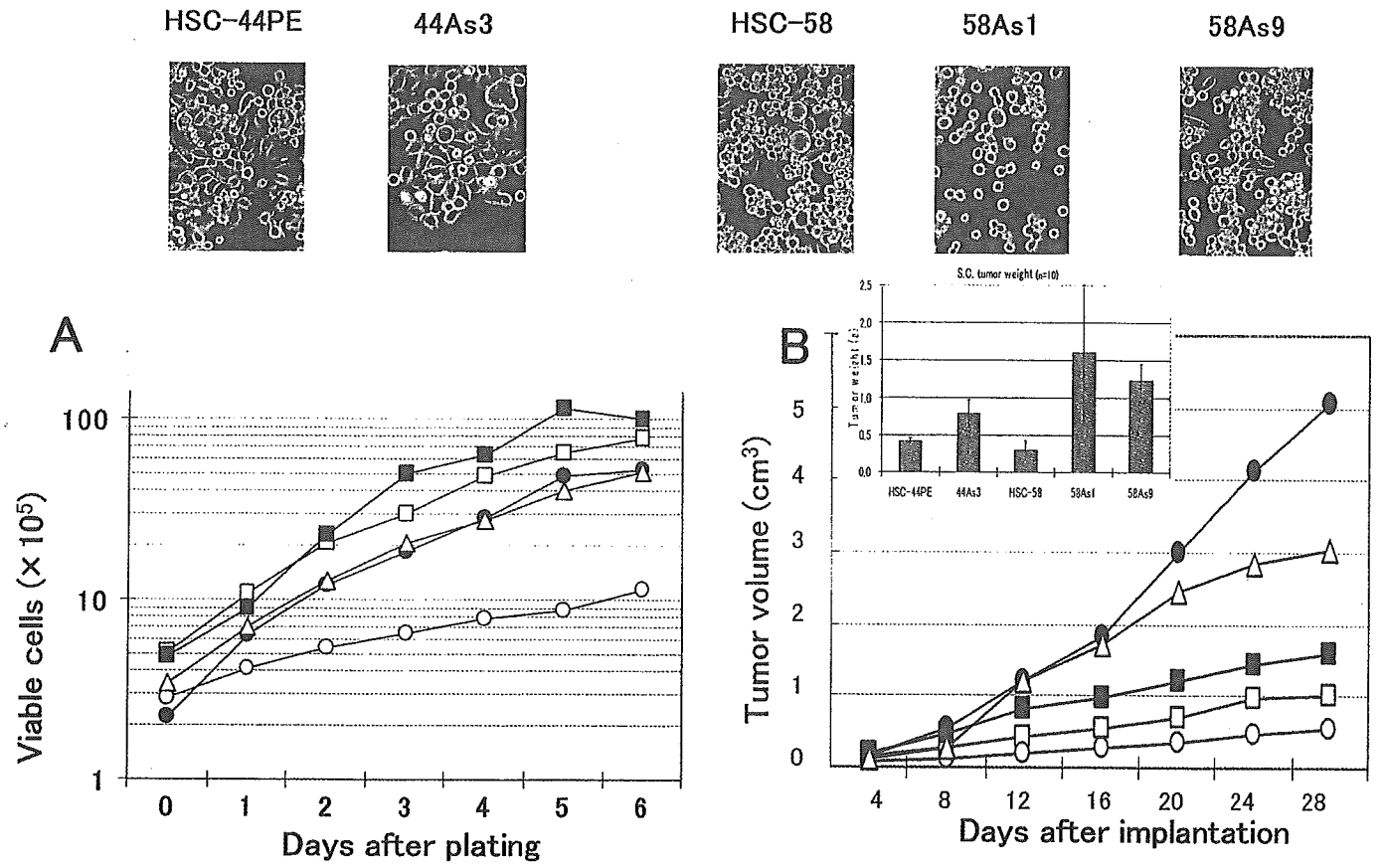

Fig. 1. Phase-contrast micrographs and the growth properties of the sublines showing a high metastatic potential and their parent cell lines. Original magnification, ×200. (A), Growth curves of the cells *in vitro*. Cells were seeded at a density of 1×10^5 cells/well in 6-well plates (Falcon, Lincoln Park, NJ, USA), and the cell numbers were determined daily. The results of a representative experiment are given and the points indicate the average of the results in 3 wells in which the cell numbers varied by 10%. (B), Growth curves of the cells *in vivo*. Tumor volume was measured at predetermined time intervals described in 'Materials and Methods.' HSC-44PE (□), 44As3 (■), HSC-58 (○), 58As1 (●), and 58As9 (△) cell lines were used. Similar results were obtained in a second experiment conducted independently.

mesenterium and so on, and caused the formation of bloody ascites in a small number of animals.[14] Following this result, we incubated the cancer cells isolated from the ascitic fluid of mice, which developed cancerous peritonitis 3–6 months following the orthotopic implantation of HSC-44PE and HSC-58 cells, and attempted orthotopic injection of the incubated cells. This sequence of manipulations was repeated for 12 cycles in an attempt to reliably isolate cell lines that would have higher potentials of undergoing metastasis (in the form of dissemination) over short periods of time. We first obtained a cell line (44As3) from HSC-44PE cells that possessed a high metastatic potential, with a strong capability of inducing ascites. The 44As3 cells resembled the parent HSC-44PE cells in their morphological characteristics. While most cells of this subline exhibited high adhesivity, a small number of spherical cells remained floating and showed proliferative activity. Occasional signet ring cells were also observed (Fig. 1). Although the proliferative potential of the 44As3 cells did not differ greatly from that of the parent cell line *in vitro* (Fig. 1A), the former induced more rapid s.c. tumor formation than the latter (Fig. 1B).

Two highly metastatic cell lines (58As1 and 58As9) were also established from the HSC-58 cells. The 58As1 cells assumed the form of aggregates of spherical cells with low adhesive capacity, which remained floating and showed proliferative activity. In contrast, 58As9 cells often exhibited high adhesivity, resembling the parent cell line, HSC-58, in this characteristic (Fig. 1). Both 58As1 and 58As9 cells exhibited higher proliferative potential *in vitro* than the parent HSC-58 cells (Fig. 1A), and the tumor-forming capability following s.c. injection of these subclones differed markedly from that of the parent cell line; the 58As1 cells, in particular, showed a markedly higher tumor-forming capability (Fig. 1B).

Comparison of the highly metastatic cell lines and the parent cell lines *in vivo*. Table 1 shows the metastatic behavior and the survival days of animals following orthotopic injection of the tumor cells. Orthotopic implantation of 44As3 cells resulted in the formation of bloody ascites approximately 20 days later, and some mice became moribund (Fig. 2D). Dissemination was most often seen to the greater omentum, mesenterium, parietal peritoneum, diaphragm, and so on. Metastasis to the regional lymph nodes and liver was also frequently seen (Table 1). Micrometastasis was observed in the pancreas (also in the lungs, although rarely). The percentage of parent HSC-44PE cells that survived at the site of implantation was 68%. Inoculation of HSC-44PE cells resulted in the animals becoming moribund approximately 85 days after the implantation, but none of the animals developed ascites (Table 1, Fig. 2D).

When 58As1 or 58As9 cells were implanted orthotopically, bloody ascites began to form approximately 3 weeks after the inoculation, accompanied by tumor dissemination to the greater omentum, mesenterium, parietal peritoneum, diaphragm and so on, and the animals died soon thereafter (Table 1, Fig. 2A–C). Lymph node metastasis was observed in all the animals; metastasis to the liver was also noted. Micrometastases were seen in the pancreas and the lungs. Implantation of 58As1 cells was followed by the development of micrometastases in the

Table 1. Metastasis and peritoneal dissemination after orthotopic inoculation of human gastric cancer cell lines and sublines†

Cell line	Survival days	Tumor formation	Ascites	Lymph node	Lung‡	Liver	Pancreas‡	Kidney‡	Disseminated Metastasis			
									Omentum	Mesenterium	Parietal peritoneum	Diaphragm
HSC-44PE	131 ± 44 (85–200)	13/19 (68%)	0/13 (0%)	5/13	0/13	0/13	0/13	0/3	4/13	3/13	2/13	0/13
44As3	33 ± 11 (20–62)	21/21 (100%)	19/21 (90%)	21/21	2/21	19/21	10/21	0/21	21/21	21/21	20/21	14/21
HSC-58	85 ± 16 (68–123)	16/20 (80%)	1/16 (6%)	5/16	1/16	3/16	1/16	0/16	6/16	3/16	3/16	0/16
58As1	32 ± 5 (23–42)	21/21 (100%)	20/21 (95%)	21/21	6/21	19/21	7/21	4/21	21/21	21/21	21/21	13/21
58As9	45 ± 13 (22–68)	14/14 (100%)	14/14 (100%)	14/14	2/14	7/14	1/14	0/14	14/14	10/14	11/14	8/14

†Mice were killed at 200 days after the orthotopic implantation. Data are shown as the number of mice bearing metastasis at the site/total number of mice bearing tumor. ‡Micrometastasis.

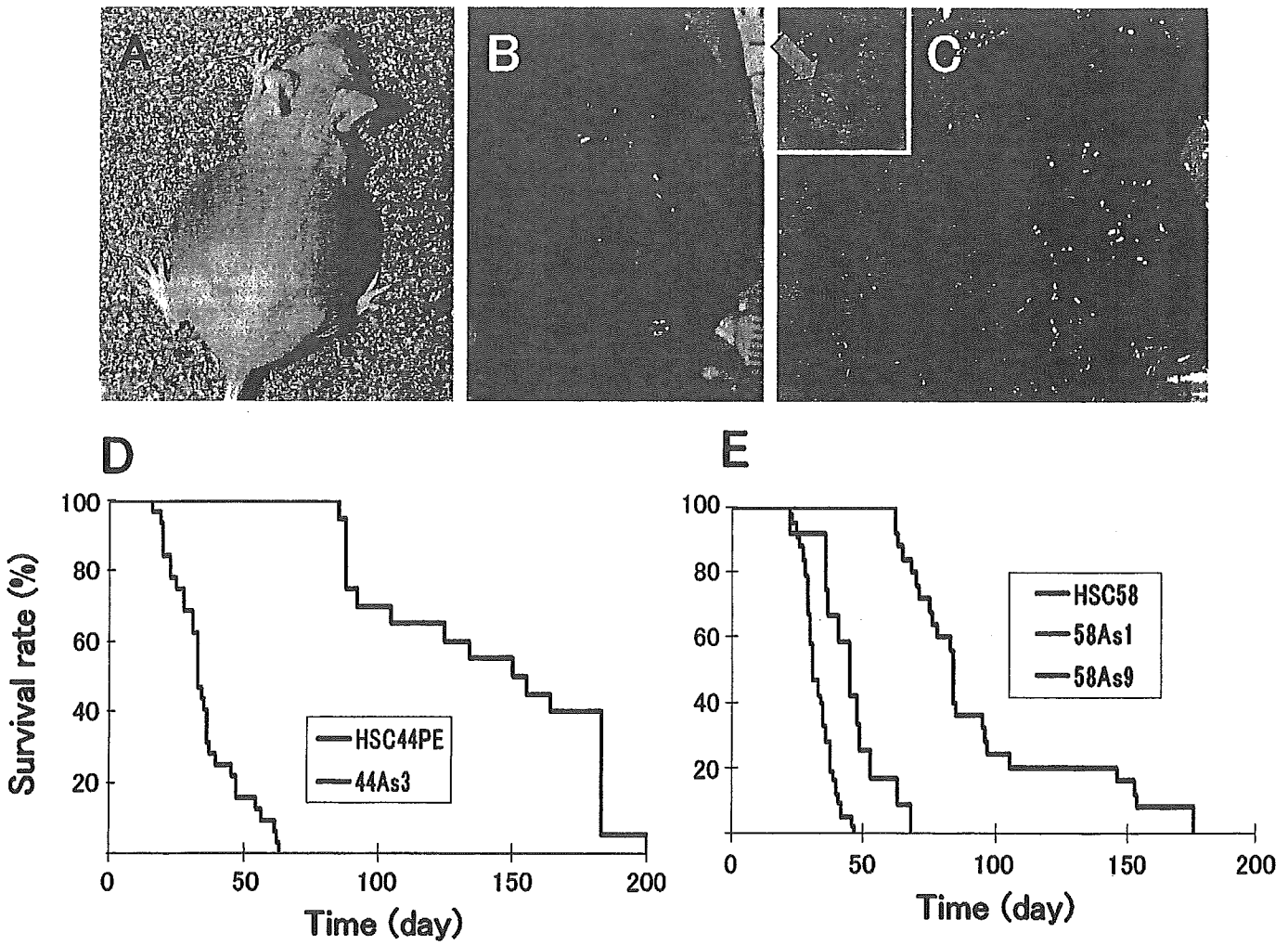

Fig. 2. Macroscopic appearance of the peritoneal disseminations, and survival of nude mice after orthotopic implantation of the cell lines. (A,B), Carcinomatous peritonitis was observed 4 weeks after orthotopic implantation of 58As1 cells. Abdominal distension because of bloody ascites was evident. (C), Peritoneal dissemination was recognized from the innumerable whitish nodules visualized in the abdominal cavity, mesenterium, omentum, parietal peritoneum and diaphragm. Orthotopic implantation of 58As1 cells in the stomach of nude mice was followed by tumor formation 3 weeks later (green arrow, inset). (D), Survival of 44As3-, and HSC-44PE-tumor-bearing mice ($n = 15$; $P < 0.001$). (E), Survival of 58As1-, 58As9-, and HSC-58-tumor-bearing mice ($n = 20$; $P < 0.001$). The experiments were repeated thrice and yielded similar results each time.

 doi: 10.1111/j.1349-7006.2005.00054.x